



Sudan University of Science and Technology
College of Graduate Studies



**Using Yukawa Potential and Method of Images to Study
Charge Distribution in Conductors**

**استخدام جهد يوكاوا وطريقة الصور لدراسة توزيع
الشحنات الكهربائية في الموصلات**

**A Graduate Project submitted For the Degree
complementary of Master (C M D) in physics**

Prepared by:

Reham Hassp Alrsool Hussain Ahmed

Supervised by:

Dr. Ali Sulaiman Mohamed

July 2019

الآية

قال الله تعالى:

(وَقُلْ اَعْمَلُوا فَسَيَرَى اللّٰهُ عَمَلَكُمْ وَرَسُولُهُ وَالْمُؤْمِنُونَ
وَسَتُرَدُّونَ اِلَى عَالَمِ الْغَيْبِ وَالشَّهَادَةِ فَيُنَبِّئُكُمْ بِمَا كُنْتُمْ
تَعْمَلُونَ)

سورة التوبة – الآية (105)

صدق الله العظيم

DEDICATE

To my father

To my mother

My brothers and sisters

To my aunt and her children

To all my friends

A CKNOWLEDGEMENT

All thanks and gratefulness is for Allah, the most gracious, the most merciful. I would like to thank the Sudan University and to express my sincere gratitude to my supervisors Dr.Ali Sulaiman Mohamed for his helpful discussion in the development of the problem.

ABSTARACT

Various methods to study the electric charge distribution on conductors were presented in details in this thesis. The electrostatic potential is mediated by potential law that varies as Yukawa potential instead of coulomb potential.

To simplify this physical problem and its solution, the method of images was used for the different way. Yukawa potentials were used to determine the position and magnitude of the image charges on different shapes of conductors.

Then the charge density distribution on these conductors was calculated. The charge density distributions on the surface of these conductors in case of Yukawa potential are plotted using Maple program and compared with the charge distribution in the case of using Coulomb law.

المستخلص

في هذه الدراسة تم تقديم بعض الطرق العلمية التي نشرت في دورات علمية متخصصة لدراسة كيفية توزيع الشحنة الكهربائية على الموصلات في حالة أن الجهد الناشئ عن الشحنة النقطية يختلف عن الجهد المحسوب بواسطة قانون التربيع العكسي لكولوم ويتغير وفق جهد يوكاوا .

كما استخدمت طريقة الصور في هذه الرسالة لدراسة توزيع الشحنة الكهربائية على الموصلات. وذلك بافتراض أن الجهد الناشئ عن الشحنة النقطية يختلف عن الجهد المحسوب بواسطة قانون التربيع العكسي لكولوم ويتغير وفق جهد يوكاوا. حيث تم استخدام جهد يوكاوا بدلاً من جهد كولوم بطريقته مختلفه في هذه الدراسة لتحديد موضع صورة الشحنة الكهربائية أولاً ومن ثم إيجاد كثافة الشحنة السطحية باشتقاق الجهد بالنسبة لوحدة المتجه العمودي.

تم تطبيق طريقة الصور لجهد يوكاوا على نماذج مختلفة من الموصلات (موصل على شكل لوح متصل بالأرض و موصل كروي متصل بالأرض و موصل كروي مشحون معزول).

بعد حساب كثافة الشحنة السطحية لكل هذه النماذج . استخدم برنامج Maple في رسم المنحنيات و مقارنة النتائج المتحصل عليه مع تلك النتائج المحسوبة باستخدام قانون التربيع العكسي لكولوم. من خلال مقارنة النتائج اتضح اهمية نموذج الصورة في تبسيط المسألة كما يمكن إيجاد كثافة الشحنة السطحية على سطح الموصلات.

Table of Contents

section	Topic	Page
	الأية	I
	Dedication	II
	Acknowledgement	III
	Abstract	IV
	Abstract In Arabic	V
CHAPTER ONE		
Introduction		
1.1	Introduction	1
1.2	The Problem	2
1.3	The Aim Of Study	3
1.4	General Method And Technical Background	3
1.5	Presentation Of The Thesis	4
CHAPTER TOW		
Photon Rest Mass And Effect Of Nonzero Mass Of Photon On Charge Distribution		
2.1	Introduction	5
2.2	The photon Rest Mass And Related Experiments	5
2.3	Effect Of Massive Photon On The Static Electric Field	9
CHAPTER THREE		
Conductors In The Electrical Field		
3.1	Introduction	11
3.2	Behavior Of Conductors In The Electrostatic Field	11
3.2.1	Charged Metal Bal	14
3.2.2	Charged Metal Wire	15
3.3	Charge Distribution On Conductive Bodies Of Arbitrary Shapes	17
3.4	Conductors	19

3.4.1	An Ideal Conductor	19
3.4.2	Type Of Conductors	19
3.4.3	Charged Conductors	20
3.4.4	Hollow Conductor	21
3.4.5	A Hollow Spherical Conductor	22
CHAPTER FOUR Charge Density On Conducting Needle		
4.1	Introduction	24
4.2	Solid Models	25
4.2.1	Ellipsoidal	25
4.2.2	Cylindrical	27
4.3	Bead Models	29
4.3.1	Fixed Charge	29
4.3.2	Fixed Position	32
4.4	Infinite Conducting Ribbon	36
4.4.1	Exact Solution	36
4.4.2	Wire Models	38
4.4.2.1	Fixed Charge	38
4.4.2.2	Fixed Position	40
CHAPTER FIVE Results And Conclusion And Recommendations		
5.1	Introduction	42
5.2	Method And Results	43
5.2.1	Method Of Images For Yukawa Potential And Grounded Spherical Conductor	43
5.2.2	Method of Images for Yukawa Potential and Insulated Charged Spherical Conductor	46
5.3	Conclusion	49
5.4	Recommendation	51
5.5	Reference	52

List of table		
Table 2.1	Shows Several Important Limits On The Photon Rest Mass m_γ	8
Table 5.1	Total Induced Surface Charge Normalized To $-q$ on Grounded Conducting Sphere and $a = 1.0$.	45

List of figures		
Figure(3.1)	A Small Cylinder Of Negligible Height With One Base In The Conductor.	14
Figure(3.2)	Segment Of an Infinitely Long Straight Wire Of Circular Cross Section Of Radius a .	16
Figure(3.3)	A Charged Metal Body	18
Figure(3.4)	Injected Charge Into The Conductor	19
Figure(3.5)	A Conductor With a Net Charge	21
Figure(3.6)	Neutral Spherical Conductor In Equilibrium With an Internal Cavity Containing a Net Charge $-q$.	22
Figure(4.1)	Conducting "Needle"	25
Figure(4.2)	Conducting Ellipsoid	26
Figure(4.3)	Conducting Cylinder	27
Figure(4.4)	Linear charge density on a conducting cylinder, using $a= 1$, $Q=1$, and $R= 0.001$	28
Figure(4.5)	Four Equal Charges on A finite Wire	28
Figure(4.6)	Charge Densities for (a) $n=5$, (b) $n=10$, and (c)	30

	n= 100.	
Figure(4.7)	Graph of Equation. (4.7) superimposed on (Figure 4.6).	31
Figure(4.8)	Four Equally Spaced Charges on A finite Wire.	32
Figure(4.9)	The 2n Evenly Spaced Charges on A finite Wire.	32
Figure(4.10)	Charge Densities Using the Fixed-Position Method: (a) n=5, (b) n=10, and (c) n=100	34
Figure(4.11)	Charge Densities using Ross' method: (a) n=5, (b) n=10, and (c) n=100	36
Figure(4.12)	Infinite Conducting Ribbon.	37
Figure(4.13)	Charge Density on A ribbon.	
Figure(4.14)	Array of Parallel Wires with Equal Charges.	38
Figure(4.15)	Surface Charge by Constant Charge Method: (a) n=5, (b) n=10, and (c) n=100.	40
Figure(5.1)	Two-dimensional schematic illustration of a conducting sphere of radius a with a point charge q outside and image charge q/inside.	43
Figure(5.2)	The surface charge density normalized to $-q/4\pi a^2$ for conducting insulated charged sphere has unit radius and $a/y=2$ is plotted as a function of angle θ .	48
Figure(5.3)	The surface charge density normalized to $-q/4\pi a^2$ for conducting insulated charged sphere has unit radius and $a/y=4$ is plotted as a function of angle θ .	48
Figure(5.4)	The magnitude of the total surface charge	49

	normalized to q and the total volume charge normalized to q , are displayed for $(Q/q = -1, y/a = 2)$ as function of k . Note that the charge conducting sphere has unit radius.	
--	--	--

Chapter One

Introduction

1.1 Introduction

Coulomb's Law is a fundamental principle describing the electric force between isolated charges, and represents the first quantitative law achieved in electromagnetism. The degree of confidence with which the law is experimentally known to hold was investigated after the law was put forth by Coulomb in 1785. The electrodynamics for massive particles suggests that a photon with a finite rest mass will cause a deviation from the inverse square law. So, modern interpretations of the possible deviation from Coulomb's inverse square law are usually associated with the non-zero photon mass. In this article, we first give a historical review of the foundation of Coulomb's inverse square law. Then, the experimental searches for validity of Coulomb's Law, particularly in its inverse square nature, are generally introduced. Based on Proca's equations, the unique.

Simplest relativistic generalization of Maxwell's equations, the link between the deviation from Coulomb's Law and the upper limit on the photon rest mass based on the concentric-spheres apparatus established in the classical experiment of Cavendish is reviewed. Up to now, all the experiments show no evidence for a positive value, and the experimental result was customarily expressed as an upper limit on the deviation or on the photon rest mass. As a representative method with the double mission of testing of the validity of Coulomb's Law and of the photon rest mass, possible improvements for this kind of experiment are discussed.

The famous inverse square law in electrostatics, first published in 1785 by Charles Augustin de Coulomb,

is known as the fundamental law of electrostatics. As the first quantitative law in the history of electricity, Coulomb's inverse square law has played a crucial role and made great contributions to the development of electricity and magnetism, and other related fields. Coulomb's Law, along with the principle of superposition, gives Gauss's Law and the conservative nature of the electric field, which may be generalized Using the Lorentz transformation to obtain Maxwell's equations. Even then, the Validity of Coulomb's Law has been tested.

Continuously over the past centuries. Based on the classical ingenious scheme Devised by Henry Cavendish [1, 2], modern experiments usually yield not only the result of possible deviation from Coulomb's inverse square law, but that of the upper limit on the photon rest mass [3, 7].

The photon, as the fundamental particle of electromagnetic interaction, is generally assumed to be mass less. This hypothesis is based on the fact that a Photon cannot stand still for ever. However, a nonzero photon mass could be so small that present-day experiments cannot probe it. Taking into account the uncertainty principle, the photon mass could be estimated using $m_\gamma \approx \hbar/(\Delta t)c^2$ to have a magnitude of about 10^{-66} g while the age of the universe is about 10^{10} years, which gives the ultimate limit for meaningful experimental measurements of the photon mass. Up to now, there is no positive result for the photon rest mass or the deviation from Coulomb's inverse square law. The experimental results just serve to set an upper bound to the photon mass and the deviation from the exponent 2 in the inverse square law. The aim of this paper is to give a review of the main ideas and results of the investigations intended to test Coulomb's Law and pertinently to improve the upper limit on the photon rest mass.

1.2 The Problem

The great triumphs of Maxwell and electromagnetism and quantum electrodynamics were based on the hypothesis that the photon should be particles with zero rest mass. The photon could carry energy and momentum from place to place and light rays would propagate in vacuum with a constant velocity c being independent of inertial frames, which was the second postulate in Einstein's theory of special relativity. As a result, the velocity of a particle with finite mass would never reach the constant c . The fact that light could not stand still made the assumption reasonable and it was difficult to find any counter-examples in theory. Still, experimental efforts to improve the limits on the rest mass of the photon in other words, to challenge the accepted theories of the time have continued since the time of Cavendish or earlier, even before the concept of the photon was introduced. So in case of nonzero photon mass the universal constant c will be different and Maxwell equation will reduce to Proca form.

1.3 The Aim Of Study

The aim of this thesis is to construct a moral idea to study charge distribution in case of potential deviating from inverse square Coulomb's law.

1.4 General Method And Technical Background

From the time of Cavendish or earlier, Coulomb's inverse square law has been tested directly or indirectly. Experiments with higher precision and involving different dimensions have been performed over the years. It is now customary to quote tests of the inverse square law in one of the following two ways [8]

- (a) Assume that the force varies with the distance r between two point charges according to the phenomenological formula $1/r^2 + q$ and quote a value or limit for q , which represents departure from the Coulomb inverse square law.
- (b) Assume that the electrostatic potential has the 'Yukawa' form $e^{-\mu_\gamma r}/r$ instead of the Coulomb form $1/r$ and quote a value or limit for μ_γ or μ_γ^{-1} . Since $\mu_\gamma \approx m_\gamma c/\Delta t$ the

test of the inverse square law is sometimes expressed in terms of an upper limit on the photon rest mass. Geomagnetic and extraterrestrial experiments give μ_γ or m_γ , while laboratory experiments usually give q and perhaps μ_γ or m_γ .

(c) Using method of images to calculate charge density and maple program to construct graphical representation.

1.5 Presentation of the thesis

This thesis contain five chapters chapter one was an introduction in chapter two Photon rest mass and effect of nonzero mass of photon on charge distribution, in Chapter three conductors in the electrical field chapter four charge density on Conducting needle chapter five results and conclusion and recommendations.

Chapter Two

Photon Rest Mass and Nonzero Mass of Photon on Charge Distribution

2.1 Introduction

The famous inverse square law in electrostatics, first published in 1785 by Charles Augustin de Coulomb, is known as the fundamental law of electrostatics. As the first quantitative law in the history of electricity, Coulomb's inverse square law has played a crucial role and made great contributions to the development of electricity and magnetism, and other related fields. Coulomb's Law, along with the principle of superposition, gives Gauss's Law and the conservative nature of the electric field, which may be generalized using the Lorentz transformation to obtain Maxwell's equations. Even then, the validity of Coulomb's Law has been tested continuously over the past centuries. Based on the classical ingenious scheme devised by Henry Cavendish [1, 2], modern experiments usually yield not only the result of possible deviation from Coulomb's inverse square law, but that of the upper limit on the photon rest mass [3, 7].

The photon, as the fundamental particle of electromagnetic interaction, is generally assumed to be mass less. This hypothesis is based on the fact that a photon cannot stand still for ever. However, a nonzero photon mass could be so small that present-day experiments cannot probe it. Taking into account the uncertainty principle, the photon mass could be estimated using $m_\gamma \approx \hbar/(\Delta t)c^2$ to have a magnitude of about 10^{-66} g while the age of the universe is about 10^{10} years, which gives the ultimate limit for meaningful experimental measurements of the photon mass. Up to now, there is no positive result for the photon rest mass or the deviation from Coulomb's inverse square law. The experimental results just serve to set an upper bound to the photon mass and the deviation from the exponent in the inverse square law.

2.2 The Photon Rest Mass and Related Experiments

The great triumphs of Maxwellian electromagnetism and quantum electrodynamics were based on the hypothesis that the photon should be a particle with zero rest mass. The photon could carry energy and momentum from place to place and light rays would propagate in vacuum with a constant velocity c being independent of inertial frames, which was the second postulate in Einstein's theory of special relativity. As a result, the velocity of a particle with finite mass would never reach the constant c . The fact that light could not stand still made the assumption reasonable and it was difficult to find any counter-examples in theory. Still, experimental efforts to improve the limits on the rest mass of the photon in other words, to challenge the accepted theories of the time have continued since the time of Cavendish or earlier, even before the concept of the photon was introduced.

A finite photon mass may be accommodated in a unique way by changing the inhomogeneous Maxwell equations to the Proca equations, the theoretical expressions of possible nonzero photon rest mass introduced by Proca [9] and de Broglie [10]. In the presence of sources ρ and J , these

Equations may be written as (SI units)

$$\nabla \cdot \mathbf{E} = \frac{\rho}{\epsilon_0} - \mu_\gamma^2 \phi \quad (2.1)$$

$$\nabla \times \mathbf{E} = -\frac{\partial \mathbf{B}}{\partial t} \quad (2.2)$$

$$\nabla \cdot \mathbf{B} = 0 \quad (2.3)$$

$$\nabla \times \mathbf{B} = \mu_0 \mathbf{J} + \mu_0 \epsilon_0 \frac{\partial \mathbf{E}}{\partial t} - \mu_\gamma^2 \mathbf{A} \quad (2.4)$$

Together with the field strengths $\mathbf{E} = -\nabla \phi - \partial \mathbf{A} / \partial t$, $\mathbf{B} = \nabla \times \mathbf{A}$ and the Lorentz condition

$$\nabla \cdot \mathbf{A} + \frac{1}{c^2} \frac{\partial \phi}{\partial t} = 0 \quad (2.5)$$

Where ϕ and \mathbf{A} are the scalar and the vector potentials, which uniquely determine the field, and $\mu^{-1} = \hbar/(m_\gamma c)$ is a characteristic length, with $m_\gamma = 0$ as the photon mass. If $m_\gamma = 0$, the Proca equations would reduce to Maxwell's equations. The Proca equations, the relativistic ally invariant modification of Maxwell's equations, provide a complete and self-consistent description of electromagnetic Phenomena [7].

In four-dimensional space the Proca equations can be rewritten as

$$(\square^2 - \mu_\gamma) \mathbf{A}_\mu = -\mu_0 \mathbf{J}_\mu \quad (2.6)$$

Table 2.1.shows several important limits on the photon rest mass m_γ .

Author (date) Ref.	Experimental scheme	Upper limit on m_γ /g
Terrestrial results		
Goldhaber et al (1971)	[4] Speed of light	5.6×10^{-42}
Williams et al (1971)	[13] Test of Coulomb's law	1.6×10^{-42}
Chernikov et al (1992)	[14] Test of Ampere's law	8.4×10^{-46}
Lakes (1998)	[15] Static torsion balance	2×10^{-50}
Luo et al (2003)	[16] Dynamic torsion balance	1.2×10^{-50}
Extraterrestrial results		
de Broglie (1940)	[10] Dispersion of starlight	0.8×10^{-39}
Feinberg (1969)	[17] Dispersion of starlight	10^{-44}
Schaefer (1999)	[18] Dispersion of gamma ray bursts	4.2×10^{-44}
Davis et al (1975)	[19] Analysis of Jupiter's magnetic field	8×10^{-49}
Fischbach et al (1994)	[20] Analysis of Earth's magnetic field	1.0×10^{-48}
Ryutov (1997)	[21] Solar wind magnetic field and plasma	10^{-49}
Gintsburg (1964)	[22] Altitude dependence of geomagnetic field	3×10^{-48}
Patel (1965)	[23] Alfvén waves in Earth's magnetosphere	4×10^{-47}
Hollweg (1974)	[24] Alfvén waves in interplanetary medium	1.3×10^{-48}
Barnes et al (1975)	[25] Hydromagnetic waves	3×10^{-50}
DeBernadis et al (1984)	[26] Cosmic background radiation	3×10^{-51}
Williams et al (1971)	[27] Galactic magnetic field	3×10^{-56}
Chibisov (1976)	[5] Stability of the galaxies	3×10^{-60}

Where A_μ and J_μ are the 4-vector of potential $(A, i\phi/c)$ and current density $(J, ic\rho)$, respectively. The d'Alembertian symbol \square^2 is equal to $\nabla^2 - \partial^2/\partial (ct)^2$. In free space, the above equation reduces to

$$(\square^2 - \mu_\gamma)A_\mu = 0 \quad (2.7)$$

Which is essentially the Klein–Gordon equation for the photon. The characteristic length scale μ_γ^{-1} , namely the reduced Compton wavelength of the photon, is an effective range in which the electromagnetic interaction would exhibit an exponential damping by $\exp(-\mu_\gamma^{-1} r)$.

2.3 Effect of Massive Photon on the Static Electric Field

Once the photon is provided with a finite mass, three immediate consequences may be deduced from the Proca equations: the frequency dependence of the velocity of light propagating in free space; the third state of the polarization direction, namely the ‘longitudinal photon’; and some modifications in the characteristics of classical static fields. All those effects are useful approaches for laboratory experiments and cosmological observations to determine the upper bound on the photon mass.

What is of interest in this paper is the effect of a massive photon in a static electric field. In the case of a massive photon, the wave equation will be modified for all potentials (including the Coulomb potential) in the form

$$\left(\nabla^2 - \frac{1}{c^2} \frac{\partial^2}{\partial t^2} - \mu_\gamma^2 \right) \phi = -\frac{\rho}{\epsilon_0} \quad (2.8)$$

For a point charge and in the static case, this yields a Yukawa type potential,

$$\phi(r) = \frac{1}{4\pi\epsilon_0} \frac{Q}{r} \exp(-\mu_\gamma r) \quad (2.9)$$

and the electric field

$$E(r) = \frac{Q}{4\pi\epsilon_0} \left(\frac{1}{r^2} + \frac{\mu_\gamma}{r} \right) \exp(-\mu_\gamma r) \quad (2.10)$$

Inspection of equations (2.8), (2.10) shows that if $r \ll \mu_\gamma^{-1} r$ then the inverse square law of forces is a good approximation, but if $r \gg \mu_\gamma^{-1} r$, then the force law departs from the prediction of Maxwell’s equations. Up to now, finding the exponential deviation from Coulomb’s Law provides the most reliable test for the photon rest mass in terrestrial experiments, in that those laboratory tests have the advantage of free variation of the experimental parameters [7]. As for large scale observations, the limits usually come from the analyses of astronomical data of the cosmological magnetic field. However, those results are essentially order-of-magnitude arguments due to the incomplete knowledge

about the structure of the large scale magnetic field [11, 12]. In section 4 will review those laboratory experiments in detail.

Chapter Three

Conductors in the Electric Field

3.1 Introduction

Conductors are in all electric devices. They are as common in electrostatics as in other areas of electrical engineering. Nevertheless, it is important to understand how they behave in electrostatics. This behavior explains some useful electromagnetic devices.

In addition, in many non-electrostatic applications conductors behave similarly to the way they do in electrostatics. So this chapter is important beyond its application to electrostatics.

3.2 Behavior of Conductors in the Electrostatic Field

Conductors have a relatively large proportion of freely movable electric charges. The best conductors are metallic (silver, aluminum, copper, gold, etc.). They usually have one free electron per atom, an electron that is not bound to its atom, but moves freely in the space between atoms. Because of their small mass, these free electrons move in response to any electric field, however small, that exists inside a conductor. The same is true for all other conductors, e.g., liquid solutions and semiconductors, except that inside such conductors both positive and negative free charges can exist. The number of free charge carriers is smaller and their mass greater than in metals and electrons, but this has no influence on the behavior of conductors in the electrostatic field.

Let us make an imaginary experiment. Assume that this book is a conductor.

Suppose that it has both free positive and negative charges in equal number. If the book is not situated in the electric field, the number of positive and negative free charge inside any small volume is the same, and there is no surplus electric charge at any point in the book. To be more picturesque, imagine that positive

charges are blue and negative yellow. If mix blue and yellow we get green, so your book will look green both over its surface and at any point inside.

What would happen if establish an electric field in the book, for example, by means of two electrodes on the two sides of the book, charged with equal charges of opposite sign. Let the positive electrode be on your left. The electric field in the book will then be directed from left to right. You would notice that blue (positive) charges move from left to right (repelled by the positive electrode), and that yellow (negative) charges move from right to left. consequently, the right side of the book will become progressively more blue (positive), and its left side progressively more yellow (negative).

The surplus charges in the body created in this manner are known as electrostatically induced charges. They are, of course, the source of an electric field. Because the positive induced charge is on the right side of the book, and the negative on its left side, this electric field is directed from right to left, i.e., opposite to the initial electric field that produced the charge. As the amount of the induced charge increases, the total field inside the book becomes progressively smaller and the motion of charges inside the book decays. In the end, the electric field of induced charges at all points inside the book cancels out the initial electric field (due to the two charged electrodes). Thus reach electrostatic equilibrium, in which there can be no electric field at any point inside our conductive book.

Form this simple imaginary experiment, we conclude the following:

if we have a conducting body in an electrostatic field, and wait until the drift motion of charges under the influence of field stops (in reality, an extremely rapid process) the electric field of induced charges will exactly cancel out the external field, and the total electric field at all points of a conductor will be zero. Thus the first fundamental conclusion is

In electrostatic $E = 0$ inside conductor (3.1)

With this knowledge, let us apply Gauss law to an arbitrary closed surface S that is completely inside the conductor. Because vector E is zero at all points on S , the total charge enclosed by S must be zero. This means that all the excess charge (if any) must be distributed over the surfaces of conductor:

In electrostatics, a conductor has charges only on its surface. Because there is no field inside conductors, the tangential component of the electric field strength, E , on the very surface of conductors is also zero (otherwise it would produce organized motion of charge on its surface):

In electrostatics, $E_{\text{tangential}} = 0$ on conductor surfaces. (3.2)

Because the tangential component of E is zero on conductor surfaces, the potential difference between any two points of a conductor is zero. This means that the surface of a conductor in electrostatics is equipotential. Because there is no E inside conductors either, it follows that all points of a conductor have the same potential.

In electrostatics, the surface and volume of a conductor are equipotential.

Finally, a simple relation exists between the normal component, E_n of E on a conductor surface, and local surface charge density, σ . To derive this relation, consider a small cylindrical surface, similar to a coin, with a base ΔS and a height $\Delta h \rightarrow 0$. One base is in the conductor and the other in air (Figure.3.1). Let us apply Gauss' law to the closed surface of the cylinder. There is no flux of E through the base inside the conductor (zero area). The flux of E through the cylinder is thus equal only to

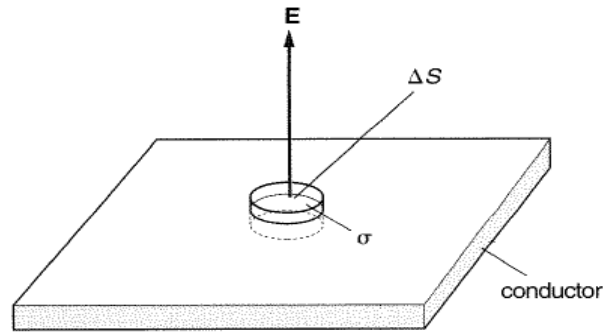


Figure.3.1 a small cylinder of negligible height with one base in the conductor.

$$E_n = \frac{\sigma}{\epsilon_0} \quad (3.3)$$

Normal component of electric field strength close to conductor surface

The simple conclusions in Equation. (3.1) through (3.3) are all need to know to understand the behavior of conductors in the electrostatic field.

3.2.1 Charged Metal Bal

Suppose that a metal ball of radius a is situated in a vacuum and has a charge Q . How will the charge be distributed over its surface [We know from Equation (3.2) that Q exists only over the conductor surface.] Because equal charges repel, due to symmetry the charge distribution over the surface of the ball must be uniform. The surface charge density is therefore simple. $\sigma = Q/4\pi a^2$ Let us determine E and V due to this charge.

Due to the uniform charge distribution, vector E is radial and has the same magnitude on any spherical surface concentric to the ball. (Is such a surface an equipotential surface). Can use Gauss' law to find the magnitude of vector E on any of these surfaces:

$$\oint_{\text{sphere}} E(r) \cdot ds = E(r)4\pi r^2 = \frac{Q}{\epsilon_0}$$

Note that the sphere encloses no charge if $r < a$. thus

$$E(r) = \frac{Q}{4\pi\epsilon_0 r^2} = \frac{\sigma 4\pi a^2}{4\pi\epsilon_0 r^2} = \frac{\sigma a^2}{\epsilon_0 r^2} (r > a),$$

$$E(r) = 0 \quad r < a \tag{3.4}$$

This expression is the same as the one for the field of a point charge Q at the center of the ball. On the surface of the ball ($r=a$), $E(a) = \sigma/\epsilon_0$ as predicted by Equation (3.3). It follows that outside the ball, the potential is the same as that of a point charge Q placed at the center of the ball. Inside the ball the potential is constant, equal to that on the ball surface, that is

$$v(a) = \frac{Q}{4\pi\epsilon_0 a} = \frac{\sigma a}{\epsilon_0} \tag{3.5}$$

3.2.2 Charged Metal Wire

Consider a very long (theoretical, infinitely long) straight metal wire of circular cross section of radius a . Let it be charged with Q' per unit length.

What are the field and potential everywhere around the wire?

Due to symmetry, the charge will be distributed uniformly over the wire surface. It is not difficult to conclude that, as the result of this symmetrical charge distribution, vector E is radial. Its magnitude depends only on the normal distance r from the wire axis and can be determined by Gauss' law.

For the application of Gauss' law, we adopt the cylindrical surface shown in Figure.3.2. There is no flux through the cylinder bases because vector E is tangential to them. The total flux through the closed surface is therefore equal to the flux through its cylindrical part. Applying Gauss' law gives

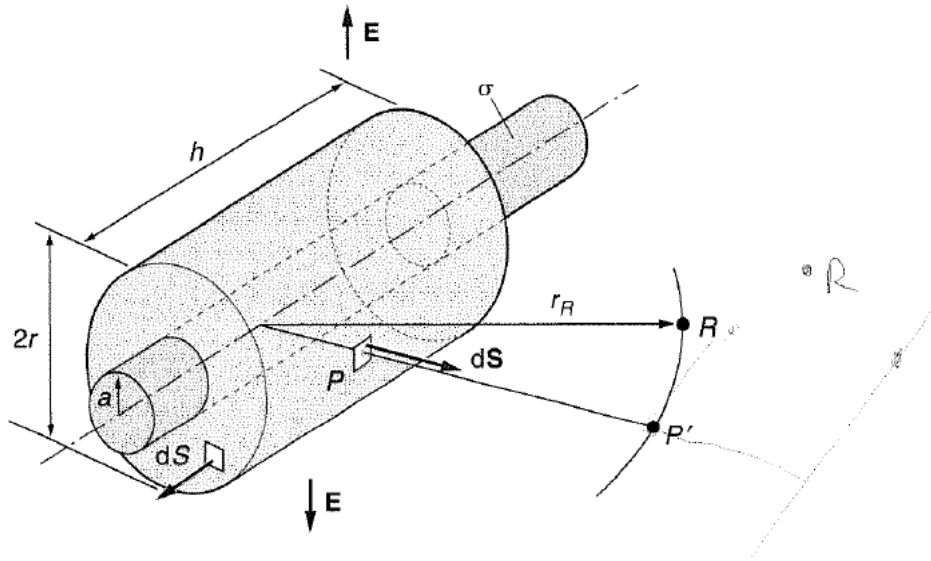


Figure.3.2.Segment of an infinitely long straight wire of circular cross section of radius a.

$$\oint_s E \cdot ds = \int_{belt} E ds = E(r)2\pi r h = \frac{Q_{in\ cylinder}}{\epsilon_0} = \frac{Q'h}{\epsilon_0}$$

Note that if $r < a$ the surface encloses no charge. Thus,

$$E(r) = \frac{Q'}{2\pi\epsilon_0 r} \quad r > a \quad , \quad E(r) = 0 \quad (r < a) \quad (3.6)$$

(Electric field of straight, infinitely long, uniformly charged thin wire)

Because the surface charge density on the cylinder is $\sigma = Q'/(2\pi a)$, $E(r)$ the wire surface can be written in the form. $E(a) = \sigma/\epsilon_0$ This of course, is the result as obtained by applying Equation (3.3).

The determination of potential is slightly more complicated consider a point P at a containing P and the wire axis. Recall that we can adopt any path from P to R in determining the potential. Choose the simplest: first a radial line from P to the distance rR from the wire axis, and then a line parallel to the axis to R, Figure.3.2. Along the first path segment, E and the line element are parallel, so $E \cdot dl = E(r)dL = E(r)dL = E(r)dr$, because the line element, dL becomes the differential increase in r , dr . Along the second path segment $E \cdot dl = 0$. Thus have

Or

$$V(r) = \int_P^R E \cdot dI = \int_r^{r_R} E(r) dr = \frac{Q'}{2\pi\epsilon_0} \int_r^{r_R} \frac{dr}{r}$$
$$V(r) = \frac{Q'}{2\pi\epsilon_0} \ln \frac{r_R}{r} \quad (3.7)$$

(Potential of straight, infinitely long, uniformly charged thin wire)

See that in this case cannot adopt the reference point at infinity, because

$\text{Log}\infty \rightarrow \infty$.

The expressions in Equations (3.6) and (3.7) are also useful for noninfinite wires, as long as we are interested in the field at points close to the wire and away from the ends. Because metallic wires are used often in electrical engineering, these equations are important.

3.3 Charge Distribution on Conductive Bodies of Arbitrary Shapes

Only for symmetrical isolated conductors is the charge distribution on their surface known actually, inferred from symmetry. For conducting bodies of arbitrary shape the determination of charge distribution is one of the most important and the most difficult problems in electrostatics. Except in a few relatively simple cases, it can be determined only numerically. For many applications, it is useful to have a rough idea what the charge distribution is like. In estimating the charge distribution, the following simple reasoning can be of significant help.

We know that on an isolated metal sphere the charge is distributed uniformly. Also know that if the radius of the sphere is a and the surface charge density on it is σ , then the potential of sphere is $V(a) = \sigma a / \epsilon_0$ (Equation 3.5). Let us use this expression to estimate the charge distribution on a more complex conducting body.

Consider a charged metal body sketched in (Figure.3.3). It consists of a larger sphere of radius a , onto which are pressed part of two smaller spheres of radii b and c .

Close to points A, B, and C indicated in the figure, the surface charge density is not the same. These three points are, however, at the same potential, V because the body is conductive. because charges that are close to a certain point predominantly contribute to the potential at the point, roughly speaking the surface charge density σ_A is approximately that of a sphere of radius a at the potential V . there for, according to Equation.(3.5) $\sigma_A \approx \epsilon_0 V/a$.Similarly, $\sigma_B \approx \epsilon_0 V/b$, and $\sigma_C \approx \epsilon_0 V/c$.Thus, for the conducting body shown in (Figure.3.3), $a\sigma_A \approx b\sigma_B \approx c\sigma_C$.

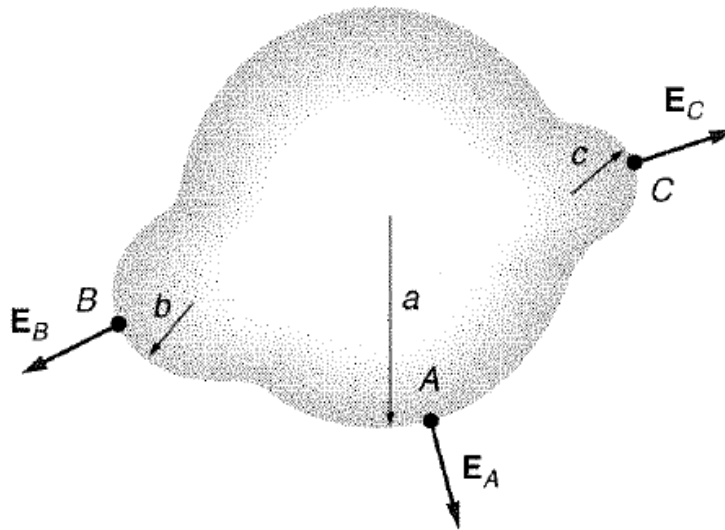


Figure.3.3. A charged metal body

Because the surfaces charge density is proportional to the local electric field strength, $aE_A \approx bE_B \approx cE_C$.

These are simple but important approximate result. They tell us that the surface charge density at different points a metal body is approximately inversely proportional to the curvature of the surface of the body at these points. This means that the largest charge density and electric field strength on charged conductive bodies is around sharp parts of the body.

An application of Equation (3.7), for example, is a simple method for discharging aircraft. During flight, the plane becomes charged due to air friction. this charge could produce large fields during landing that in turn could produce a spark resulting in parts, the charge density and, consequently, the electric field at these points become very high and the air ionizes(i.e., becomes conductive). A large portion of the charge "leaks" through these conducting channels into the atmosphere.

3.4. Charged Conductors

Now suppose inject charge into the conductor. Since like charges repel, the injected charges will move as far away from each other as possible, without leaving the conductor. This implies that the charge must reside on the surface of the conductor. Moreover, the field within the conductor must be zero. Because the conductor is in equilibrium. By definition, this means that there is no net migration of charge. If there is no net migration of charge, this implies that the free charges experience a net electric force of zero, that is, zero electric field.

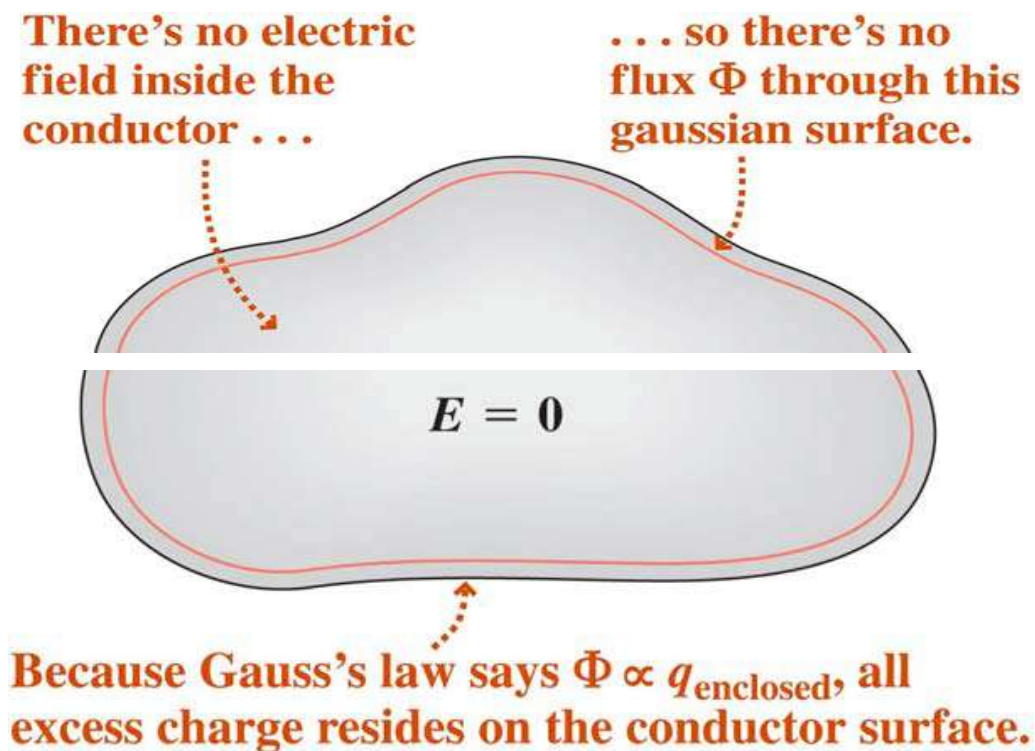


Figure.3.4 Injected Charge into the Conductor

3.4.1 A Hollow Conductor

Consider a conductor with a net charge of $+1 \mu\text{C}$. As noted, the charges will migrate rapidly to the surface of the conductor and distribute themselves in such a way that the electric field within the conductor is zero. Suppose that the cavity within the conductor contains a $+2 \mu\text{C}$ charge. Because the field within the conductor is zero, the field on the Gaussian surface shown is necessarily zero. Therefore, according to Gauss's law, the net charge enclosed by the Gaussian surface must also be zero.

The only way the net charge enclosed by the Gaussian surface can be zero is if, in addition to the $+2\mu\text{C}$ in the cavity, there is also within the Gaussian surface a charge of $-2\mu\text{C}$. It comes from the free charges in the conductor, which are attracted to the $+2\mu\text{C}$ charge. In the only place it can: on the inner surface of the conductor. Moreover, the inner surface charge is distributed so that its field plus that of the $+2\mu\text{C}$ charge sum to zero, as it must, outside the cavity, that is, within the conductor.

But since the net charge of the conductor is $+1\mu\text{C}$, and its inner surface has a charge of $-2\mu\text{C}$, it follows from charge conservation that a charge of $+3\mu\text{C}$ must exist somewhere in or on the conductor. A net charge cannot reside in a conductor in equilibrium. Nor can it reside on the inner surface, because if it did the net charge there would be $-2\mu\text{C} + 3\mu\text{C} = 1\mu\text{C}$, contradicting Gauss's law. Therefore, the $+3\mu\text{C}$ charge must reside on the conductor's outer surface.

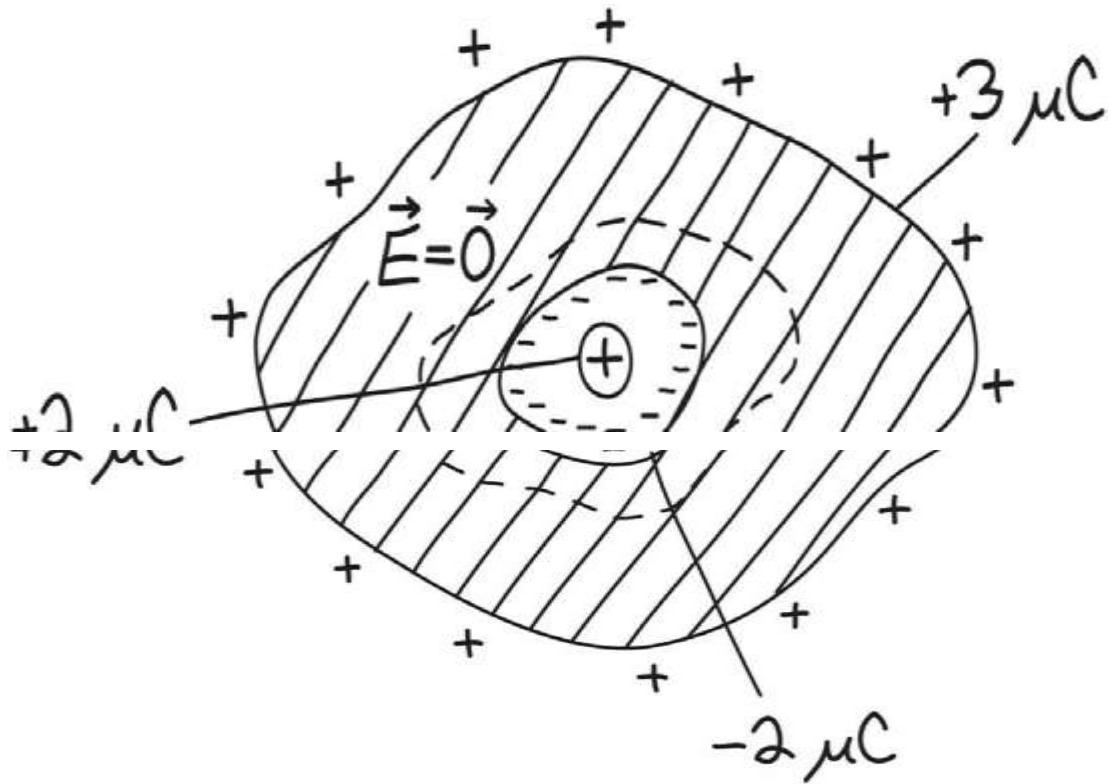


Figure.3.5 a conductor with a net charge

3.4.2 A Hollow Spherical Conductor

Consider a neutral spherical conductor in equilibrium with an internal cavity containing a net charge $-q$. The fact that the conductor is neutral means that its net charge is zero.

1. The charge on the inner surface of the cavity is $+q$.
2. The charge on the outer surface of the conductor must therefore be $-q$.
3. Amazingly, in this case, this charge is uniformly distributed. Because the inner surface charge exactly cancels the field in the conductor due to the charge in the cavity and, consequently, the conductor behaves exactly like a neutral spherical conductor without a cavity.

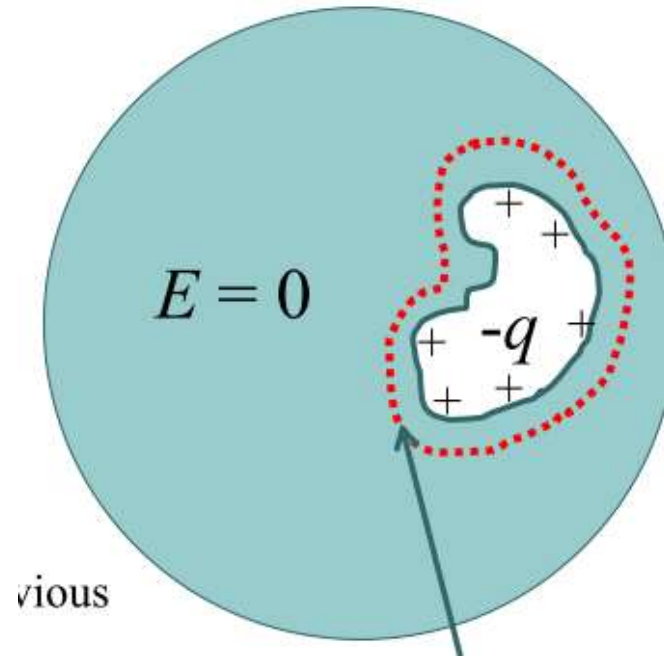


Figure.3.6. Neutral spherical conductor in equilibrium with an internal cavity containing a net charge $-q$.

Chapter Four

Charge Density on Conducting Needle

4.1 Introduction

Imagine a straight of conducting wire, length $2a$, on which place an electric charge Q (Figure.4.1). Question: in the absence of external fields, how will the charge distribute itself along the wire That is, what is the equilibrium linear charge density; it seems obvious that coulomb repulsion will push charge out toward the ends, just as the charge on a solid conductor flows to the surface. However, it is not clear how much of the charge goes to the ends; presumably some of it is left spread out along the length of the "needle."

The question sounds simple enough, and it must surely have been considered long ago by Sommerfeld, Smythe, Stratton, or maybe even Maxwell himself. However, we have found no reference to it in the literature. The reason may be that the problem as it stands is ill posed: the answer apparently depends on the particular model used to represent the needle. If we think of it as a solid object, we are obliged to specify its profile: is it (say) an elongated ellipsoid (Section 4.2.1), or is it perhaps a thin circular cylinder (Section. 4.2.2) As we shall see, these two cases lead to radically different results, and the differences seem to persist even in the limit as the number of beads goes to infinity (and the charge on each one goes to zero). Alternatively, we might model the system as a collection of charged "beads" on a string stretched between $-a$ and $+a$ (see. 4.3.1). Can solve for their equilibrium positions, and examine the limit as the number of beads goes to infinity (and the charge on each one goes to zero). Or might put the beads at fixed locations along the string, and solve for the equilibrium partitioning of the total charge (Section.4.3.2). Will these two "bead" models yield the same effective linear charge density To what solid shape (if any) do they correspond Unfortunately, for more than four beads it is prohibitively difficult to perform the calculations analytically, and we must

resort to numerical methods. [However, if substitute a Hook's law interaction for the true Columbic one, the problem is exactly soluble.]

In this paper we explore each of these models: solids in (Section.4.2) and beads in (Section.4.3). After that, as a sort of "reality check," it is instructive to compare the two-dimensional analog: the charge density on an infinite conducting "ribbon" (of width $2a$ and infinitesimal thickness). This problem has the virtue that it is well defined and exactly soluble, so the methods applied earlier to the needle can be put to rigorous test (Section.4.4). In the concluding section (Section.4.5), we summarize our results, and return to the question of what this problem really means.

4.2 Solid Models

4.2.1 Ellipsoidal

The charge density on an ellipsoidal conductor

$$\frac{x^2}{a^2} + \frac{y^2}{b^2} + \frac{z^2}{c^2} = 1 \quad (4.1)$$

With total charge Q is [28]

$$\sigma = \frac{Q}{4\pi abc} \left(\frac{x^2}{a^4} + \frac{y^2}{b^4} + \frac{z^2}{c^4} \right)^{-\frac{1}{2}} \quad (4.2)$$

Here $a, b,$ and c are the three semi-axes (Figure.4. 2).

To calculate the total charge dQ on a ring of width dx , note that an element of area dA on the surface is related to its projection in the xz plane by

$$dx dz = \cos\theta dA \quad (4.3)$$

Where θ is the angle between the y axis and the unit vector \hat{n} normal to the surface:

$$\cos\theta = \hat{j} \cdot \hat{n}' \quad (4.4)$$

Now, \hat{n} can be calculated by taking the gradient of $f(x, y, z) = \left(\frac{x}{a}\right)^2 + \left(\frac{y}{b}\right)^2 + \left(\frac{z}{c}\right)^2$

and dividing off its length

$$\hat{n}' = \left(\frac{x^2}{a^4} + \frac{y^2}{b^4} + \frac{z^2}{c^4} \right)^{-\frac{1}{2}} \left(\frac{x}{a^2}, \frac{y}{b^2}, \frac{z}{c^2} \right) \quad (4.5)$$

Thus

$$\cos\theta = \frac{y}{b^2 \sqrt{x^2/a^4 + y^2/b^4 + z^2/c^4}} \quad (4.6)$$

Evidently the charge on a patch of surface above $dx dz$ is

$$\sigma dA = \frac{Q}{4\pi ac} \frac{1}{y} dx dz \quad (4.7)$$

The total charge on the ring is four times the charge on one quadrant:

$$dQ = \frac{Qb}{\pi ac} dx \int_0^{c\sqrt{1-x^2/a^2}} \frac{1}{y} dz$$

(4.8)

From Equation (4.1) we have

$$y = b\sqrt{\left(1 - \frac{x}{a}\right)^2 - \left(\frac{z}{c}\right)^2} \quad (4.9)$$

The integral simplifies if we let $u \equiv z/c\sqrt{1 - (x/a)^2}$

$$dQ = \frac{Q}{\pi a} dx \int_0^1 \frac{du}{\sqrt{1-u^2}} = \frac{Q}{2a} dx \quad (4.10)$$

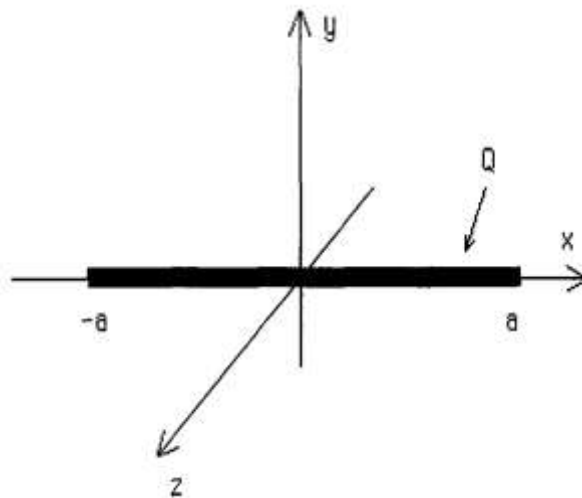


Figure.4.1. conducting "needle"

Astonishingly, the effective line charge $\lambda(x) = dQ/dx$ is constant [29]

$$\lambda(x) = Q/2a \tag{4.11}$$

Since this result is independent of b and c , it holds in the limit $b, c \rightarrow 0$ when the ellipsoid collapses to a line segment along the x axis. Conclusion: If the needle is the limiting case of an ellipsoid, then the linear charge density is constant. In this case the tapering of the ends exactly cancels the tendency for charge to push out toward the extremities.

4.2.2. Cylindrical

The exact charge distribution on a conducting cylinder is not known. In his pioneering study, Smythe [30] remarks that “the literature is blank on this subject;” Taylor [31] adds that the problem “must be regarded as intractable from the point of view of conventional methods.” A number of authors have extended and improved Smythe's preliminary results [32], but the limiting case of zero radiuses remains elusive.

Smythe begins by expressing the surface charge density on the ends (σ_e) and on the sides (σ_s) in the form of two series:

$$\sigma_s(x) = \sum_{n=0}^{\infty} A_n (a^2 - x^2)^{n-1/3}$$

$$\sigma_e(r) = \sum_{n=0}^{\infty} B_n (R^2 - r^2)^{n-1/3}$$

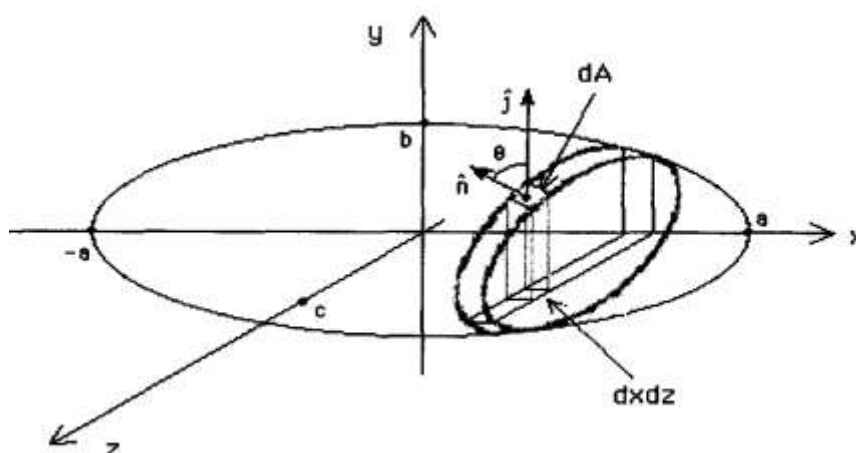
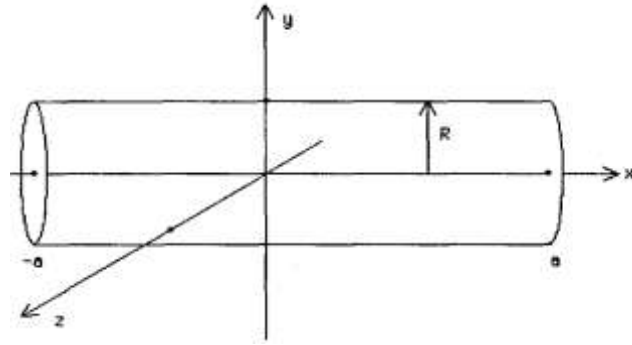


Figure.4.2. Conducting Ellipsoid.



Figuer.4.3. Conducting Cylinder.

Where R is radius of cylinder (Figure.4.3). (The functional form of the singularity at the “corners” is dictated by a general theorem [33]: it goes like $\delta^{-1/3}$ where δ is the distance from the edge. Smyth's ansatz simply incorporates this structure in a power series expansion.) An approximate solution is obtained by truncating the sums at $n=r$ and $n=s$, respectively. Smythe provides an algorithm for determining the coefficients A_n and B_n and a criterion for choosing the optimal values of r and s , for a prescribed degree of accuracy. He applies the technique to particular values of the aspect ratio $b \equiv a/R$ ranging from $\frac{1}{4}$ up to 4, but he does not explore the large- b regime that concerns us here.

In truth, smythe's method is not well suited to our problem. It is pretty clear that we need only one term in the B series, and off-hand one would suppose that the larger r is the better. However, in practice the calculation is wildly unstable, and many of smythe's own numbers (obtained with the aid of a desk calculator) are incorrect. Taylor refined smythe's method, using a slightly different series that converges more rapidly. Applying Taylor's technique, with $b=1000$ and $r=10$, obtained the linear charge density plotted in (Figure.4.4). This graph appears to confirm our intuition that a portion of charge pushes out to the two ends, leaving the density relatively flat toward the middle.

However, Djordjevic, drawing on extensive numerical studies using a quite different approach, reports that the charge density on a long conducting cylinder is essentially constant [$\lambda(x) = Q/2a$] over the entire rod, except in the

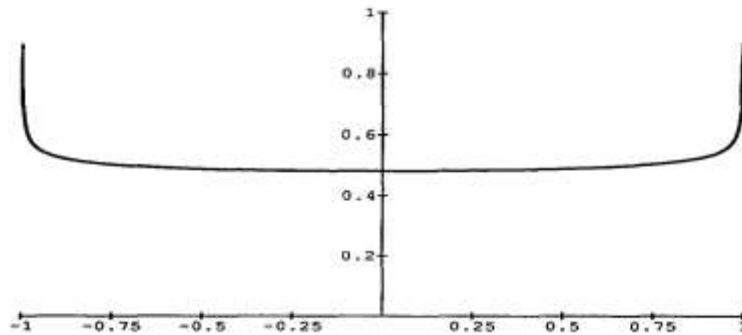


Figure.4.4. Linear charge density on a conducting cylinder, using $a= 1$, $Q=1$, and $R= 0.001$.

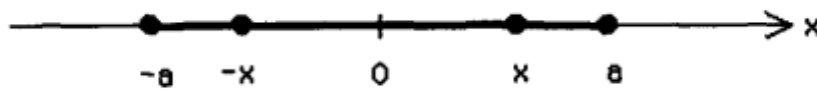


Figure. 4.5. Four Equal Charges on A finite Wire.

Immediate vicinity of the two ends; the length d of the regions over which it deviates significantly is proportional to R (specifically, $d \approx 5R$), and the total charge on these two end caps is proportional to R/a . If Djordjevic is right, then the charge density in the limit $R \rightarrow 0$ is constant for the entire cylinder, as it is for the ellipsoid.

4.3. Bead Models

4.3.1. Fixed Charge

Suppose we place $2n$ equal point charges ($q=Q/2a$) on the line from $x= -a$ to $x=a$. Our task is finding their equilibrium positions. If $n=1$, the two charges will obviously repel out to the ends. However, for $n=2$ the problem is already

nontrivial. The outermost pair will be at $\pm a$; let $\pm x$ denote the position of the other two (Fig.5). The force on the charge at $+x$ is

$$F = \frac{q^2}{4\pi\epsilon_0} \left(\frac{1}{(x+a)^2} + \frac{1}{(2x)^2} - \frac{1}{(a-x)^2} \right) \quad (4.12)$$

Setting F equal to zero yields a quartic equation:

$$(a^2 - x^2)^2 = 16ax^3 \quad (4.13)$$

To which the numerical solution is

$$x = 0.36148a \quad (4.14)$$

In general, the $2n$ charges are at $\pm(x_1, x_2, \dots, x_{n-1}, x_n \equiv a)$, and the force on the i th charge is

$$F_i = \frac{q^2}{4\pi\epsilon_0} \left(\sum_{j=1}^n \frac{1}{(x_i + x_j)^2} + \sum_{j=1}^{i-1} \frac{1}{(x_i - x_j)^2} - \sum_{j=i+1}^n \frac{1}{(x_j - x_i)^2} \right) \quad (4.15)$$

Setting $F_i = 0$ (for $i=1, 2, \dots, n-1$) yields $n-1$ coupled equations for the equilibrium positions of the charges. For example, with $n=6$ (12 charges), we find

$$X_1 = 0.10010a,$$

$$X_2 = 0.29913a,$$

$$X_3 = 0.49441a,$$

$$X_4 = 0.68241a,$$

$$X_5 = 0.85692a,$$

However, what we really want is not so much the position of each charge as the effective charge density, $\lambda(x)$. To this end we compute

$$\lambda(\bar{x}_i) = \frac{q}{x_{i+1} - x} \quad (4.16)$$

Where

$$\bar{x}_i \equiv \frac{1}{2}(x_{i+1} + x_i) \quad (4.17)$$

Is the center of the interval. The resulting plots (using $Q=1$ and $a=1$) for $n=5, 10,$ and $100,$ are shown in Figure 4.6.

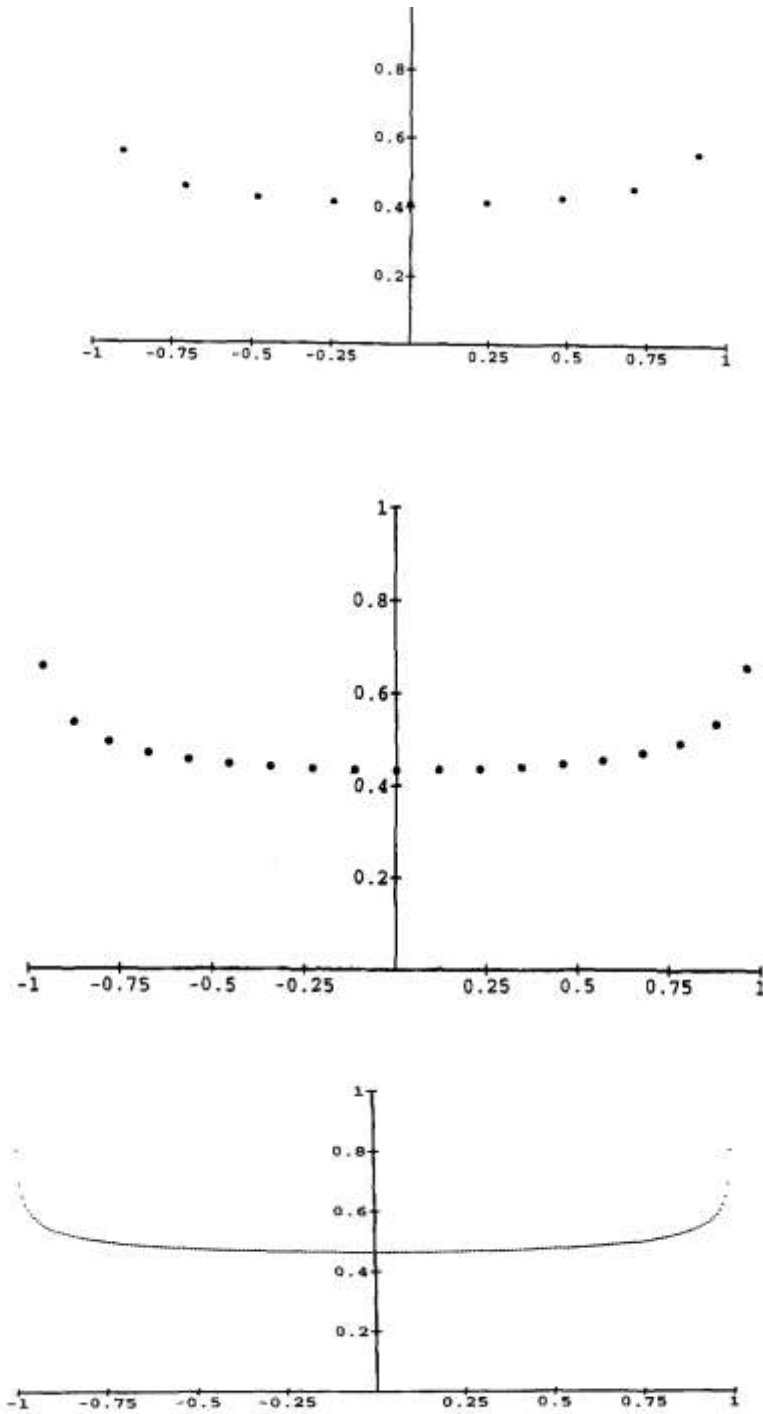


Figure 4.6. Charge Densities for (a) $n=5$, (b) $n=10$, and (c) $n= 100$.

Graphs appear to converge as n increases, suggesting that there is a well-defined limit function as $n \rightarrow \infty$. Indeed, an expression of the form

$$\lambda(x) = A + \frac{B}{(a^2 - x^2)^{1/3}}$$

(Inspired by Smythe's treatment of the finite cylinder) fits the results quite well (see Figure.4.7), if $A=0.384985$ and $B = 0.083684$. However, we have no theoretical justification for this form, no ab initio means for calculating the parameters A and B, and, in fact, no real assurance that the graphs converge at all.

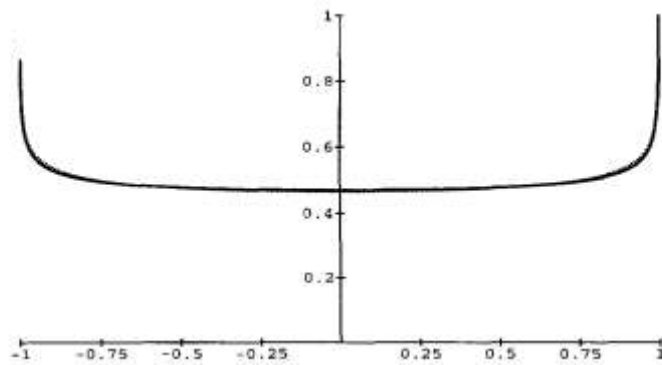


Figure.4.7. Graph of Equation. (4.7) superimposed on(Figure 4.6).

4.3.2. Fixed position

The previous model is algebraically cumbersome because the variables we seek (the positions of the charges) appear quadratically, and in the denominator. Even for the simplest (nontrivial) case ($n=2$) this led to a quartic Equation (4.12).

An alternative model, in which fix the positions of the particles and let their charges vary, yields a system of linear equations.

For example, with four evenly spaced beads there are two distinct charges:

q_1 at $\pm a/3$, and q_2 at $\pm a$ (Figure.4.8). In equilibrium, the net electrical force on q_1 (at $a/3$) is zero - the force to the left (due to q_2 at a) balances the force to the right (due to q_2 at $-a$ and q_1 at $-a/3$):

$$\frac{1}{4\pi\epsilon_0} \left(\frac{q_1 q_2}{d^2} \right) = \frac{1}{4\pi\epsilon_0} \left(\frac{q_1 q_2}{(2d)^2} + \frac{q_1 q_2}{d^2} \right) \quad (4.18)$$

Where $d = 2a/3$ is the separation between the charges. It follows that

$$q_2 = \frac{1}{4} q_2 + q_1; \quad (4.19)$$

On the other hand, the sum of all the charges is Q , so

$$q_1 + q_2 = Q/2. \quad (4.20)$$

Solving, we find

$$q_1 = \frac{3}{14} Q, \quad q_2 = \frac{2}{7} Q \quad (4.21)$$

Similarly, for $n=3$ we obtain

$$q_1 = \frac{3725}{26242} Q, \quad q_2 = \frac{1980}{13121}, \quad q_3 = \frac{2718}{13121} Q \quad (4.22)$$

In general, for $2n$ charges a distance $d = 2a/(2n-1)$. Apart, there are n unknowns, q_1, q_2, \dots, q_n (Figer.4.9). The force on charge q_i is

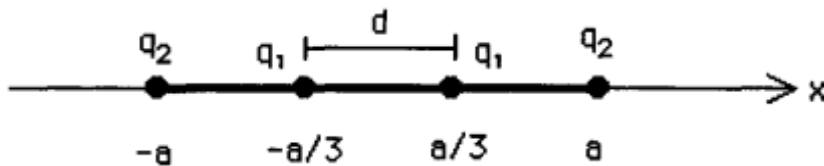


Figure.4.8. Four Equally Spaced Charges on A finite Wire.

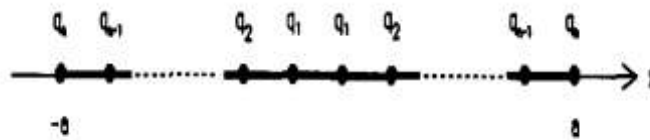


Figure.4.9. The $2n$ Evenly Spaced Charges on A finite Wire.

$$F_i = \frac{q_i}{4\pi\epsilon_0} \left(\sum_{j=1}^n \frac{q_j}{(i+j-1)^2 d^2} + \sum_{j=1}^{i-1} \frac{q_j}{(i-j)^2 d^2} - \sum_{j=i+1}^n \frac{q_j}{(j-i)^2 d^2} \right) \quad (4.23)$$

In equilibrium $F_i = 0$, so

$$\sum_{j=1}^n \frac{q_j}{(i+j-1)^2} + \sum_{j=1}^{i-1} \frac{q_j}{(i-j)^2} - \sum_{j=i+1}^n \frac{q_j}{(j-i)^2} = 0$$

Where $i=1,2,3,\dots,n-1$ (q_n , of course, is subject to the extra constraining force of the wire). Meanwhile, the total charge is Q :

$$\sum_{i=1}^n q_i = \frac{Q}{2} \quad (4.24)$$

Taken together, (4.22) and (4.23) provide n simultaneous linear equations for the n unknowns. The corresponding charge density is

$$\lambda(x_i) = \frac{q_i}{d} = \frac{n-1/2}{a} q_i \quad i=1,\dots,n, \quad (4.25)$$

Where $x_i = (i-1/2)d$. The resulting plots for $n=5, 10$, and 100 are shown in Figure 4.10. Again the graphs appear to converge as n increases and to the same function as before (compare Figures 4.6 and 4.10).

An interesting variant on this approach is suggested by the work of Ross. Instead of adjusting the charge distribution so as to make the force on each charge vanish, we require that the potentials be equal at point midway between the charges. The potential at point $d/2$ to the left of q_i is

$$v_i = \frac{1}{4\pi\epsilon_0} \left(\sum_{j=1}^n \frac{q_j}{(i+j-3/2)d} + \sum_{j=1}^n \frac{q_j}{(i-j-1/2)d} - \sum_{j=1}^{i-1} \frac{q_j}{(j-i-1/2)d} \right) \quad (4.26)$$

Letting, $\phi = 4\pi\epsilon_0 v d$ where V is the common potential, we obtain n linear equations,

$$\sum_{j=1}^n \frac{q_j}{(i+j-3/2)} + \sum_{j=1}^n \frac{q_j}{(i-j-1/2)} - \sum_{j=1}^{i-1} \frac{q_j}{(j-i-1/2)} \quad (4.27)$$

$$\phi = 0, \quad i=1,\dots,n$$

Which, together with (4.23), determine the $n + 1$ unknowns (q_1, \dots, q_n, ϕ) . For example, when $n=2$ we find $q_1 = (2/9)Q, q_2 = (5/18)Q$. IN Finguer.4.11 we graph the charge densities for $n=5, 10,$ and 100 ; the agreement again convergence to a common shape.

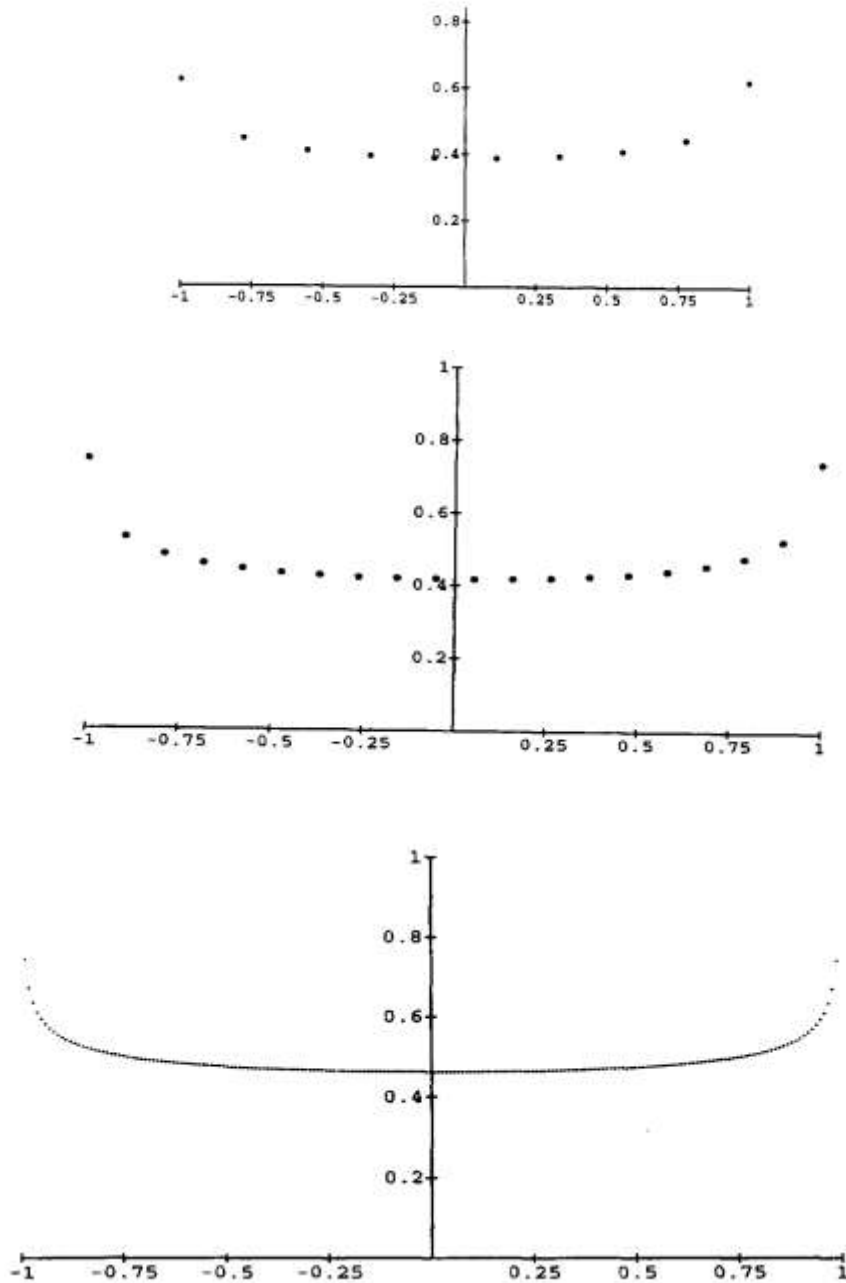


Figure.4.10. Charge Densities Using the Fixed-Position Method: (a) $n=5$, (b) $n=10$, and (c) $n=100$.

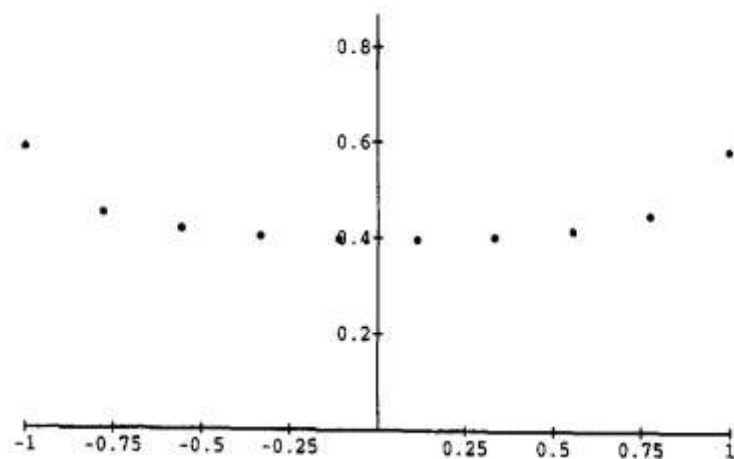
4.4. Infinite Conduction Ribbon

4.4.1. Exact Solution

The analogous case of an infinite conducting ribbon, of width $2a$ and infinitesimal thickness (Figure.4.12), can be solved exactly. For this is a strictly two-dimensional problem (the potential is plainly independent of z), and hence accessible to the method of conformal mapping. If A is the net charge per unit length (in the z direction), the potential $V(x,y)$ is given (implicitly) by the equation

$$\frac{x^2}{a^2 \cosh^2(v/v_0)} + \frac{y^2}{a^2 \sinh^2(v/v_0)} = 1 \quad (4.28)$$

Where



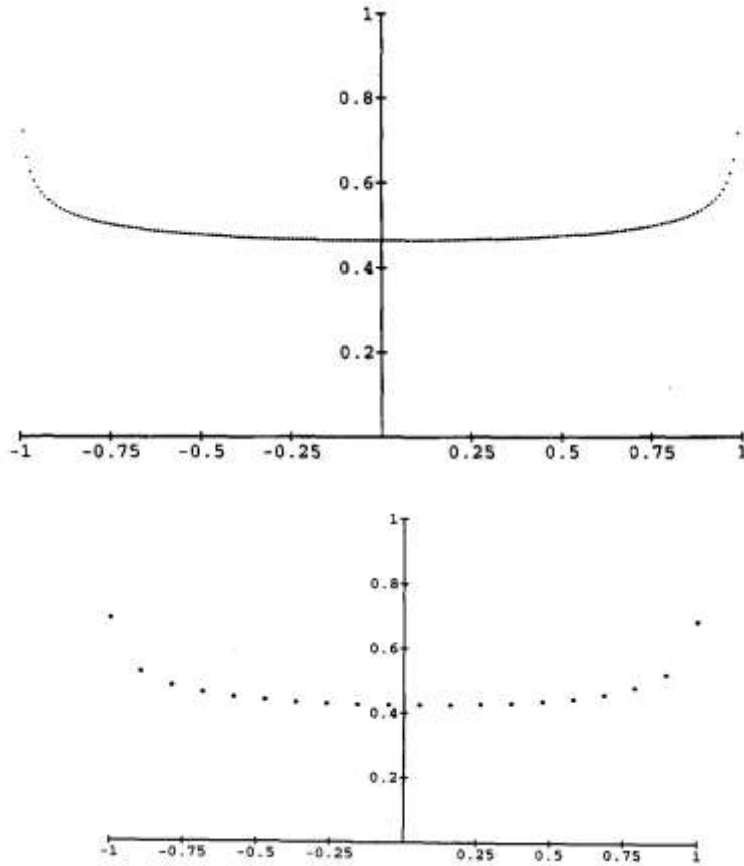


Figure.4.11. Charge Densities using Ross' method: (a) $n=5$, (b) $n=10$, and (c) $n=100$.

$$V = \frac{A}{2\pi\epsilon_0} \quad (4.29)$$

Equipotential are ellipses, with semi-axes $a \cosh(v/v_0)$ and $a \sinh(v/v_0)$. As $V \rightarrow 0$ they collapse to a line, $-a < x < +a$, along the x axis. (In this problem it is convenient to set the potential equal to 0 on the conductor.)

The charge density on the ribbon is determined by the discontinuity in the normal derivative of V :

$$\sigma(x) = -\epsilon_0 \left(-\left. \frac{\partial v_{above}}{\partial y} \right|_{y=0} - \left. \frac{\partial v_{below}}{\partial y} \right|_{y=0} \right) \quad (4.30)$$

For very small y , on the interval $-a < x < a$ (Where V is also very small) Equation (4.27) reduces to

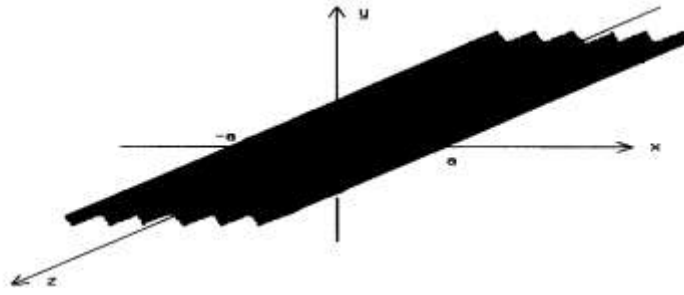


Figure.4.12. Infinite Conducting Ribbon.

$$v(x, y) \approx -\frac{v_0}{\sqrt{a^2 - x^2}}|y|, \quad (4.31)$$

So

$$\left. \frac{\partial v_{above}}{\partial y} \right|_{y=0} = -\left. \frac{\partial v_{below}}{\partial y} \right|_{y=0} = -\frac{v_0}{\sqrt{a^2 - x^2}} \quad (4.32)$$

And hence

$$\sigma(x) = \frac{A}{\pi\sqrt{a^2 - x^2}} \quad (4.33)$$

This is the exact charge density on a conducting ribbon - the, analog to the formula that has remained so elusive in the case of the needle. It is plotted in (Figure 4.13) (for $A=1$ and $a=1$). As expected, the charge is repelled out toward the edges of the ribbon.

4.4.2. Wire Models

4.4.2.1. Fixed Charge

Consider an array of $2n$ infinite wires running parallel to the z axis in the x_z plane, free to move in the x direction between $-a$ and $+a$ (Figure.4.13). If each wire carries the same linear charge density λ , what are their equilibrium positions $\pm(x_1, x_2, \dots, x_n \equiv a)$? The force per unit length on the i th wire is

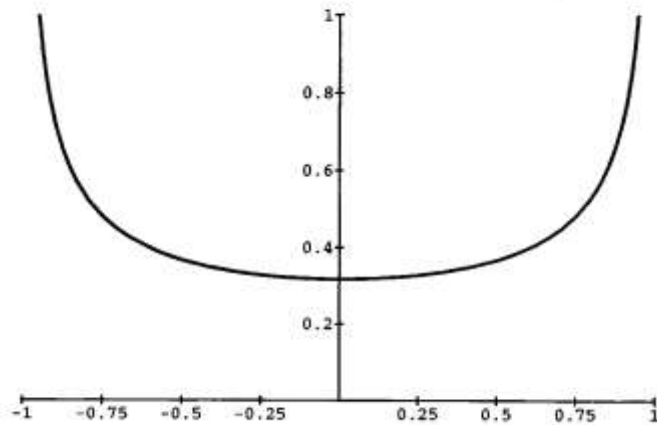


Figure.4.13. Charge Density on A ribbon.

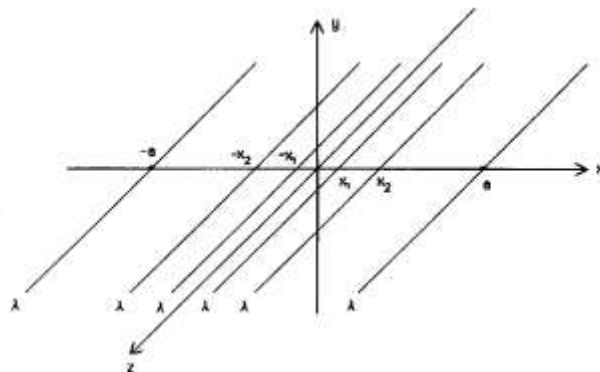


Figure.4.14. Array of Parallel Wires with Equal Charges.

$$F_i = \frac{\lambda^2}{2\pi\epsilon_0} \left(\sum_{j=1}^n \frac{1}{x_i + x_j} + \sum_{j=1}^{i-1} \frac{1}{x_i - x_j} - \sum_{j=1}^n \frac{1}{x_j - x_i} \right) \quad (4.34)$$

Setting f_i equal to 0 (for $i=1,2,\dots,n-1$) yields $n-1$ equations for the equilibrium positions of the wires. For example, if $n=2$ we find $x_1 = (a/\sqrt{5}) = 0.447a$; if $n=3$, then $x_1 = (a/\sqrt{3})^{\frac{1}{2}} = 0.285a$ and $x_2 = (a/\sqrt{a}) \left(1 + 2/\sqrt{7}\right)^{\frac{1}{2}} = 0.765a$.

We are interested in the effective surface charge $\sigma(x)$, in the limit $n \rightarrow \infty$ before,

$$\sigma(\bar{x}_i) = \frac{\lambda}{x_{i+1} - x_i} \quad (4.35)$$

With $\lambda = A/2n$

$$\bar{x}_i = \frac{1}{2}(x_{i+1} + x_i). \quad (4.36)$$

In (Figure.4.15) we plot numerical solutions for $n=5, 10,$ and 100 . The results fit the exact solution (4.32) very well.

4.4.2.2. Fixed Position

Suppose now that the wires are evenly spaced, a distance $d = (2a/2n - 1)$ apart, but their charges $(\lambda_1, \lambda_2, \dots, \lambda_n)$ are variable (Figure.4.16). The force per unit length on the i th wire is

$$f_i = \frac{\lambda_i}{2\pi\epsilon_0 d} \left(\sum_{j=1}^n \frac{\lambda_j}{i+j-1} + \sum_{j=1}^{i-1} \frac{\lambda_j}{i-j} - \sum_{j=i+1}^n \frac{\lambda_j}{j-i} \right) \quad (4.37)$$

At equilibrium $f_i = 0$, from which it follows that

$$\lambda_i = (2i-1)^2 \sum_{j \neq i}^n \frac{\lambda_j}{(j-i)(i+j-1)}, \quad i = 1, 2, \dots, n-1 \quad (4.38)$$

This gives us $n-1$ equations in n unknowns- the remaining constraint is

$$\sum_{i=1}^n \lambda_i = \frac{A}{2} \quad (4.39)$$

For example, if $n = 2$, we obtain $\lambda_1 = A/6 = 0.166 A$, $\lambda_2 = A/3 = 0.333 A$; if $n = 3$, $\lambda_1 = (31/290)A = 0.107 A$, $\lambda_2 = (18/145)A = 0.124 A$, $\lambda_3 = (39/145)A = 0.269 A$. In Figure 4.17 the resulting surface charge $\sigma(x)$ is plotted for $n=5, 10,$ and 100 ; again, the graphs are in close agreement with the exact answer.

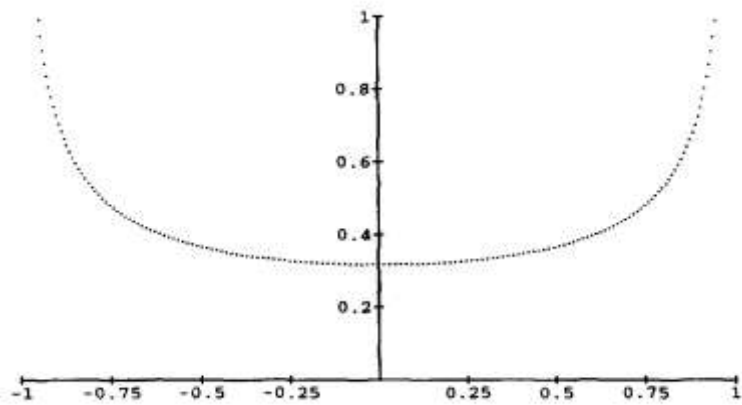
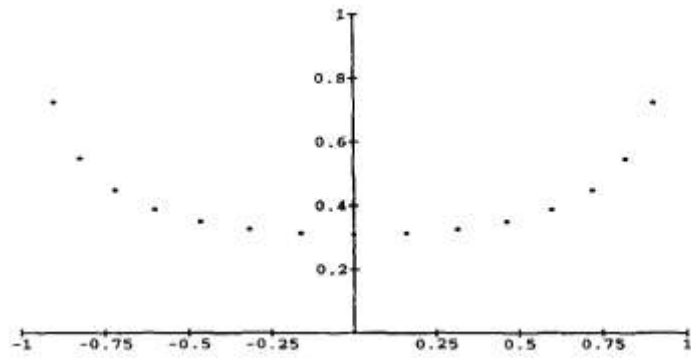
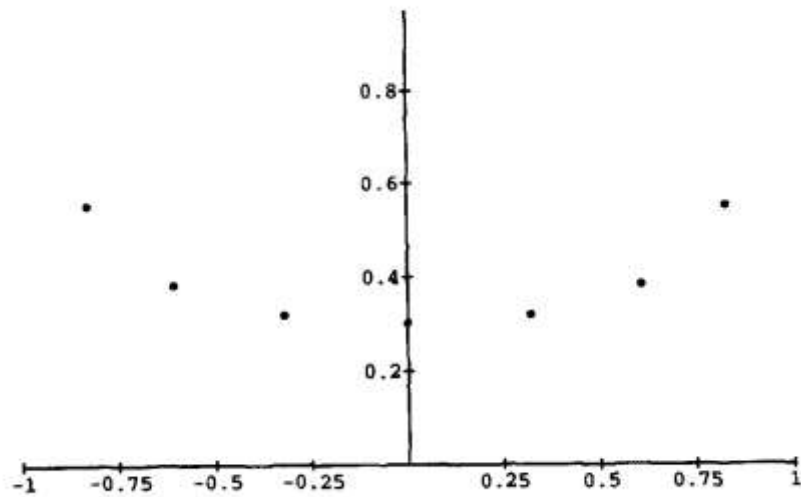


Figure.4.15. Surface Charge by Constant Charge Method: (a) $n=5$, (b) $n=10$, and (c) $n=100$.

Chapter Five

Result and Conclusion and Recommendation

5.1 Introduction

One of the foundations of electrostatics is Coulomb's law. Major electromagnetic laws are built upon this law. As a direct consequence of this law (or its equivalent, Gauss's law), any excess charge placed on a conductor must lie entirely on its surface. According to Coulomb's law, excess charges given to a conductor will move away from each other and distribute themselves about the conductor in such a manner as to reduce the total amount of repulsive forces within the conductor and that both the charge and the field inside the conductor will vanish [34], [39].

Testing this law has been a subject for many experiments over the past two and a half centuries [34], [35]. Any deviation from inverse square law would suggest a finite range for electromagnetic force, implying a nonzero photon rest mass. Rest mass of the photon provides indirect test of the deviations from exactness of Coulomb's law. If the photon mass is zero, Coulomb's inverse-square law is the foundational law in electrostatics. Experiments measure deviations in the exponent of inverse-square law and photon rest mass are increasingly exact. The most recent ion interferometry experiment measures the value of the exponent to be a few times 10^{-22} and detect a photon rest mass at the level of 9×10^{-50} grams [34]. Detection of any deviation from Coulomb's law would have far-reaching implications. Maxwell's equations and much of the standard model would have to be modified. The notion that absolute electrostatic potential is arbitrary would have to be abandoned, along with many other tenets of classical electromagnetism [34].

In an interesting papers, Spencer [36] and Griffiths and Uvanovic [37] studied distribution of excess charge within a conductor for laws rather than inverse

square law such as Yukawa's law or power law. In these two cases they found that some of the charge goes to the surface, and the remainder distributes itself uniformly over the volume of the conductor.

In this paper we introduce the method of images to study the distribution of charges in cases where the potential is depending on the photon rest of mass. And give a theoretical extension work to the experimental results that detect a photon rest mass at the level of 9×10^{-50} grams and as a result a deviating from Coulomb's Law. This paper is also important to understand physics of molecules and electron transport through a single molecule which offers a highly promising new technology for the production of electronic chip.

5.2 Method and Results

5.2.1 Method of Images for Yukawa Potential and Grounded Spherical Conductor

The reaction field of a point charge due to surrounding medium can be represented by the method of image charge. The method of images allows us to solve certain differential form of electric potential problem without specifically solving a differential equation of this problem.

The potential $\Phi(x)$ everywhere outside a conducting sphere can be calculated by using method of images. As illustrated Figure.5.1 we consider conducting sphere with radius $R = a$. For convenience, place the sphere at the origin. We assume a point charge q outside the sphere and defined by position vector y . By symmetry, the image charge lie on the line connecting the charge and the origin of the sphere and will be located inside the sphere at position vector y . If the sphere is grounded then the potential everywhere on the sphere equal zero.

Now we are able to calculate the magnitude and the position vector y of an image charge q' that is required to make the potential equal zero on the surface of the grounded sphere. Total Yukawa potential [37] $\Phi(x)$ due to the

assumed charge q and its image charge q' at any point P is given by Equation (5.1).

$$\Phi(x) = \frac{q \exp(-k|x-y|)}{|x-y|} + \frac{q' \exp(-k|x-y'|)}{|x-y'|} \quad (5.1)$$

If the sphere is grounded, then the potential at the surface of the sphere vanishes

$\Phi(x = a) = 0$, thus:

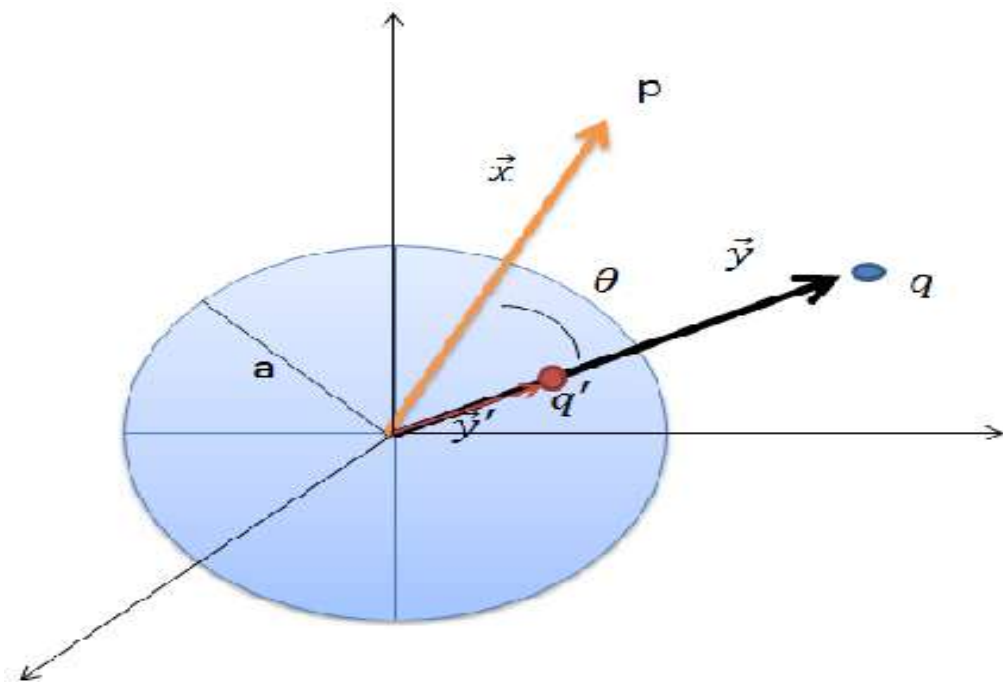


Figure.5.1. Two-dimensional schematic illustration of a conducting sphere of radius a with a point charge q outside and image charge q' inside.

$$\phi(|x|=a) = \frac{q \exp\left[-ka\left|\hat{n} - \frac{|y|}{a}\hat{n}'\right|\right]}{a\left|\hat{n} - \frac{|y|}{a}\hat{n}'\right|} + \frac{q' \exp\left[-k|y|\left|\hat{n} - \frac{a}{|y|}\hat{n}\right|\right]}{|y|\left|\hat{n}' - \frac{a}{|y|}\hat{n}\right|} \quad (5.2)$$

Where \hat{n} and \hat{n}' are unit vectors in the direction of x and y respectively. To satisfy the boundary condition

$\Phi(x) = 0$ at $R = a$, we must have:

$$q' = -\frac{a}{y} q \exp(-k|\bar{x} - \bar{y}| + k|\bar{x} - \bar{y}'|) \quad (5.3)$$

More generally, the potential in the neighborhood of an uncharged grounded conducting sphere is given by Equation (5.3):

$$\phi(\bar{x}) = q \exp(-k|\bar{x} - \bar{y}|) \left[\frac{1}{|x - y|} - \frac{a}{y} \frac{1}{|x - y'|} \right] \quad (5.4)$$

Let

$$\rho = |x - y| = (x^2 + y^2 - 2xy \cos \theta)^{\frac{1}{2}} \quad (5.5)$$

$$\rho' = |x - y'| = (x^2 + y'^2 - 2xy' \cos \theta)^{\frac{1}{2}}$$

Substitute Equation (5.5) in Equation (5.4) and then differentiate to get the actual induced charge density on the surface of the grounded uncharged conducting sphere:

$$\sigma = -\frac{1}{4\pi} \frac{\partial \Phi}{\partial x} \Big|_{x=a}$$

Let

$$\Omega = (2a - 2y \cos(\theta))$$

$$\Lambda = \left[a^2 + \frac{a^4}{y^2} - \frac{2a^3 \cos(\theta)}{y} \right]$$

$$\Gamma = (a^2 + y^2 - 2ay \cos(\theta))$$

Then we get:

$$\sigma = \frac{-5qk(\Omega) \exp(-k(\Gamma)^{\frac{1}{2}})}{(\Gamma)^{\frac{1}{2}}} \times \left[\frac{1}{(\Gamma)^{\frac{1}{2}}} - \frac{a}{y(A)^{\frac{1}{2}}} \right] + q \exp\left[-k(\Gamma)^{\frac{1}{2}}\right] \times \left[\frac{-\frac{1}{2}(\Omega)}{(\Gamma)^{\frac{3}{2}}} + \frac{1}{2}a \left[a \frac{\left[\frac{2a - 2a^2 \cos\theta}{y} \right]}{y(A)^{\frac{3}{2}}} \right] \right]$$

The total charge on the sphere may be found by integrating Equation (5.6) over all angles. The total surface induced charge is equal to the magnitude of the image charge for Coulomb potential. But in case of Yukawa potential the total surface induced charge is less than the value of the image charge. This result implies that small portion of the induced charge distributed itself inside the volume of the conducting sphere. The rest of the induced charge is distributed itself on the surface of the conducting sphere. Some values of the total induced surface charge on grounded conducting sphere are given in Table 5.1 for both Coulomb and Yukawa potentials.

Table 5.1. Total induced surface charge normalized to $-q$ on grounded conducting sphere and $a = 1.0$.

Potential	Parameters				
	K	a/y	q'	Total surface charge	Total volume charge
Coulomb	0	2.0	0.50000q	0.5	0.0
Yukawa	0.008	2.0	0.49697q	0.4932	0.0037
Yukawa	0.5	2.0	0.34592q	0.2267	0.1192
Yukawa	1.0	2.0	0.23931q	0.1087	0.1306

5.2.2. Method of Images for Yukawa Potential and Insulated Charged Spherical Conductor

We can generalize Equation (5.4) for an insulated conducting sphere. Consider insulated charged sphere with total charge Q in the presence of a point charge q . The potential $\Phi(x)$ everywhere outside the sphere

is superposition of Equation (5.4) Yukawa potential of a point charge $(Q - q)$ at the center of the conducting sphere, charge q and image charge q' is given Equation (5.7):

$$\phi(\bar{x}) = \frac{q \exp(-k\rho)}{\rho} - \frac{a}{y} \frac{q \exp(-k\rho)}{\rho'} + \frac{\left[Q + \frac{a}{y} q \exp(-k(\rho - \rho')) \right] \exp(-k\rho)}{x} \quad (5.7)$$

The surface charge density:

$$\sigma = - \frac{1}{4\pi} \frac{\partial \Phi}{\partial x} \Big|_{x=a}$$

$$\sigma(\theta) = \frac{-q}{4\pi} \frac{a}{y} (\sigma_1 - \sigma_2 + \sigma_3) \quad (5.8)$$

Where

$$\sigma_1(\theta) = \frac{-0.5k(\Omega) \exp(-k\Gamma^{0.5})}{\Gamma} - \frac{0.5(\Omega) \exp(-k\Gamma^{0.5})}{\Gamma^{1.5}}$$

$$\sigma_2 = \frac{-0.5k(\Omega) \exp(-k\Gamma^{0.5})}{y\Gamma^{0.5}z} - \frac{0.5a \left[2a - \frac{2a^2 \cos(\theta)}{y} \right] \exp(-k\Gamma^{0.5})}{yz^3}$$

$$\sigma_3 = \frac{1}{y} \left[\left[-\frac{0.5k(\Omega)}{\rho} + \frac{0.5k \left[2a - \frac{2a^2 \cos(\theta)}{y} \right]}{z} \right] \Theta \exp(-ka) \right] - \frac{\left[\frac{Q}{q} + \frac{a\Theta}{y} \right] k \exp(-ka)}{a} - \frac{\left[\frac{Q}{q} + \frac{a\Theta}{y} \right] \exp(-ka)}{a^2}$$

Where

$$\Theta = \exp(-k\rho + kz), z = \left[1 + \left[\frac{a}{y} \right]^2 - 2 \frac{a^3}{y} \cos\theta \right]^{\frac{1}{2}}$$

The charge density given by Equation (5.8) in units of $-q/4\pi a^2$ is plotted in Figures 5.2 and 5.3 as a function of the angle θ for different values of k , a/y and Q/q . The total surface charge, for insulated charged sphere with total charge Q , is calculated by integrating Equations (5.8) with respect to all angles. For $k = 0$,

we find that the total surface charge is equal to the magnitude of the total charge of (Q). This means that all the charge is distributed on the surface of the conducting sphere and no charge is distributed inside the sphere. For values of k different from zero ($k > 0$), we found that portion of the total charge is distributed inside the volume of the sphere. In Figure 4, the magnitude of the total surface charge normalized to q and the total volume charge normalized to q for insulated charged sphere with total charge Q , are displayed for ($Q/q = -1, a/y = 2$) as a function of k . Note that the charged conducting sphere is insulated in this case and has a unit radius a .

5.3. Conclusion

In accord with the experimental work we show that the charge distribution greatly depends on the photon rest

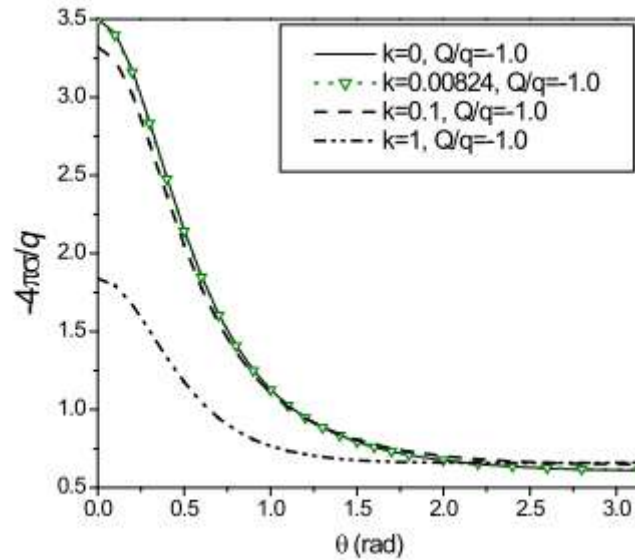


Figure 5.2. The surface charge density normalized to $-q/4\pi a^2$ for conducting insulated charged sphere has unit radius and $a/y = 2$ is plotted as a function of angle θ .

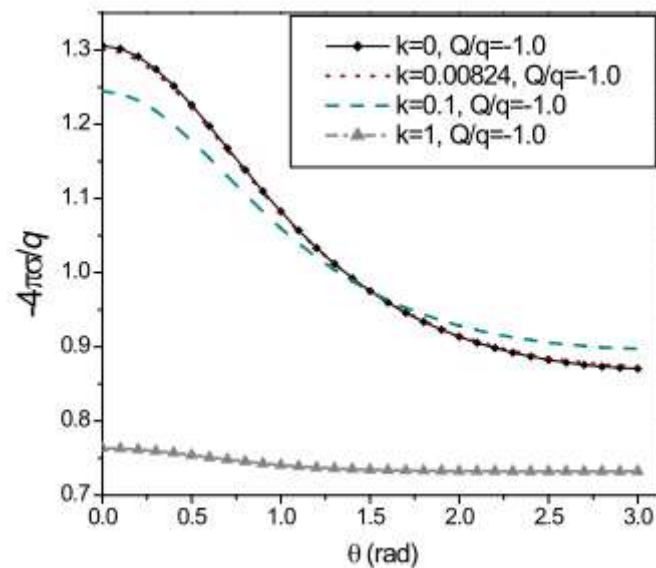


Figure 5.3. The surface charge density normalized to $-q/4\pi a^2$ for conducting insulated charged sphere has unit radius and $a/y = 4$ is plotted as a function of angle θ .

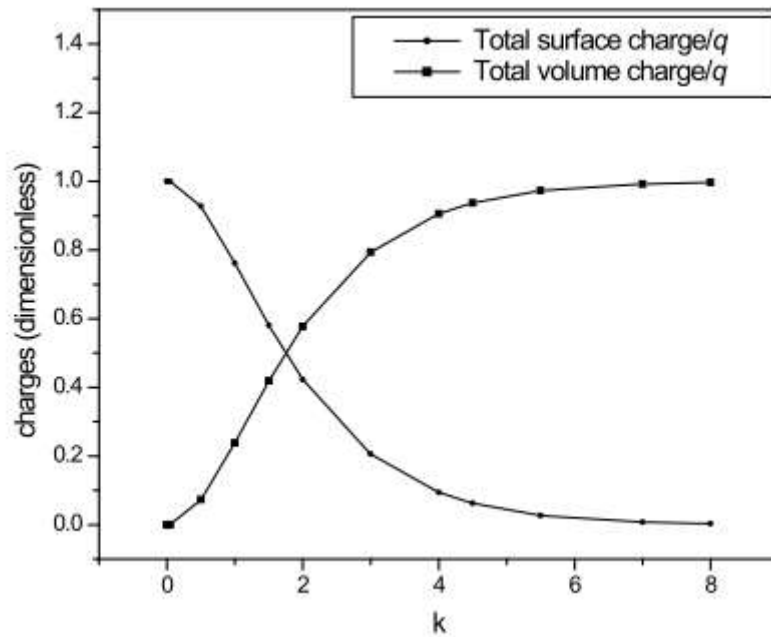


Figure.5.4. The magnitude of the total surface charge normalized to q and the total volume charge normalized to q , are displayed for $(Q/q = -1, y/a = 2)$ as function of k . Note that the charge conducting sphere has unit radius.

From which it concluded that

If photons have nonzero mass there will be many consequences:

- a. Speed of light will not be the universal constant.
- b. Coulombs Law will deviate from the inverse square law.
- c. Maxwell equation will reduce to proca equation.

5.4 Recommendation

1. More experimental work should be held in order to find the upper limit of photon mass.
2. The sensitivity of the equipment which are used to determine the photon mass must be modified to determine the mass of photon accurately.

البرنامج المستخدم في رسم المنحنيات

اولا في حالة لوح موصل (يوكاوا و كولوم)

```
with(plots):
```

```
k:=1.;
```

1.

```
d:=1.0;
```

1.0

```
A:=plot((k/(r^2+d^2)+1.0/(r^2+d^2)^1.5)*exp(-  
k*(r^2+d^2)^0.5),r=0..5,symbolsize=2,thickness=2,color=red,sym  
bol=circle,legend="yukawa k=1.0 d=1");
```

```
B:=plot(1.0/(r^2+d^2)^1.5,r=0..5,color=blue,thickness=1,symbol=  
diamond,legend="couolomb k=0 d=1");
```

```
display(A,B);
```

ثانيا في حالة كرة موصلة متصل بالأرض (يوكاوا و كولوم)

```
with(plots):
```

```
k:=0.00824;
```

k := 0.00824

ay:=1.0/2.0;

ay := 0.5000000000

a:=1.0;

a := 1.0

y:=a/2.0;

y := 0.5000000000

z:=(1.25-cos(theta))^0.5;

0.5

z := (1.25 - cos(theta))

A:=plot(k*(ay-cos(theta))*(exp(-k*(y-a)*z)-exp(-k*y*z))-k*(1-(ay)*cos(theta))*(exp(-k*(y-a)*z))/(1+(ay)^2-2.0*(ay)*cos(theta))+(1-(ay)*cos(theta))*(exp(-k*(y-a)*z))-ay*(ay-cos(theta))*(exp(-k*y*z))/(1.0+(ay)^2-2.*(ay)*cos(theta))^1.5,theta=0..Pi,color=red):

ay:=1.0/4.0;

ay := 0.2500000000

y:=a/4.0;

y := 0.2500000000

z:=(17.0/16.0-(0.5)*cos(theta))^0.5;

0.5

$$z := (1.062500000 - 0.5 \cos(\theta))$$

```
B:=plot(k*(ay-cos(theta))*(exp(-k*(y-a)*z)-exp(-k*y*z))-k*(1-  
(ay)*cos(theta))*(exp(-k*(y-a)*z))/(1+(ay)^2-  
2.0*(ay)*cos(theta))+(1-(ay)*cos(theta))*(exp(-k*(y-a)*z))-ay*(ay-  
cos(theta))*(exp(-k*y*z))/(1.0+(ay)^2-  
2.*(ay)*cos(theta))^1.5,theta=0..Pi,color=black):
```

```
ay:=1.0/2.0;
```

```
ay := 0.5000000000
```

```
a:=1.0;
```

```
a := 1.0
```

```
y:=a/2.0;
```

```
y := 0.5000000000
```

```
C:=plot(ay*(1.-ay^2)/(1.+ay^2-  
2.*ay*cos(theta))^1.5,theta=0..Pi,color=blue):
```

```
ay:=1.0/4.0;
```

```
ay := 0.2500000000
```

```
a:=1.0;
```

```
a := 1.0
```

```
y:=a/4.0;
```

```
y := 0.2500000000
```



```

d:=plot(ay*(1.-ay^2)/(1.+ay^2-  

2.*ay*cos(theta))^1.5,theta=0..Pi,color=green):  

display(A,B,C,d);

```

ثالثا في حالة كرة موصلة مشحونة و معزولة (يوكاوا و كولوم)

```
> with(plots):
```

```
> ay:=1.0/2.0;
```

```
0.5000000000
```

```
> k:=0.00824;
```

```
0.00824
```

```
> a:=1.0;
```

```
1.0
```

```
> y:=a/2.0;
```

```
0.5000000000
```

```
> Qq:=0.0;
```

```
0.
```

```
> z:=(1.25-cos(theta))^0.5;
```

```
(1.25 - cos(θ))0.5
```

```
> A:=plot(ay*(1.0-ay^2)/(1+ay^2-2.*ay*cos(theta))^1.5-  

(Qq+ay),theta=0..Pi):
```

```
> B:=plot(k*(ay-cos(theta))*(exp(-k*(y-a)*z)-exp(-k*y*z))-k*(1-  

(ay)*cos(theta))*(exp(-k*(y-a)*z))/(1+(ay)^2-
```

```
2.0*(ay)*cos(theta))+(1-(ay)*cos(theta))*(exp(-k*(y-a)*z))-ay*(ay-  

cos(theta))*(exp(-k*y*z))/(1.0+(ay)^2-2.*(ay)*cos(theta))^1.5+(-
```

```
k*(ay-cos(theta))+k*(1-ay*cos(theta))*exp(-k(y-a)*z)/z-1.0*exp(-  
k(y-a)*z),theta=0..Pi):
```

```
> display(A,B);
```

```
> k:=0.00824;
```

```
0.00824
```

```
> ay:=1.0/2.0;
```

```
0.5000000000
```

```
> a:=1.0;
```

```
1.0
```

```
> y:=a/2.0;
```

```
0.5000000000
```

```
> z=(1.25-cos(theta))^0.5;
```

```
 $(1.25 - \cos(\theta))^{0.5} = (1.25 - \cos(\theta))^{0.5}$ 
```

```
> Qq:=-1.0;
```

```
-1.0
```

```
> A:=plot(ay*(1.0-ay^2)/(1+ay^2-2.*ay*cos(theta))^1.5-  
(Qq+ay),theta=0..Pi):
```

```
> B:=plot(k*(ay-cos(theta))*(exp(-k*(y-a)*z)-exp(-k*y*z))-k*(1-  
(ay)*cos(theta))*(exp(-k*(y-a)*z))/(1+(ay)^2-  
2.0*(ay)*cos(theta))+(1-(ay)*cos(theta))*(exp(-k*(y-a)*z))-ay*(ay-  
cos(theta))*(exp(-k*y*z))/(1.0+(ay)^2-2.*(ay)*cos(theta))^1.5+(-  
k*(ay-cos(theta))+k*(1-ay*cos(theta))*exp(-k(y-a)*z)/z-1.0*exp(-  
k(y-a)*z),theta=0..Pi):
```

```
> display(A,B);
```

```
> k:=0.00824;
```

0.00824

> ay:=1.0/2.0;

0.5000000000

> a:=1.0;

1.0

> y:=a/2.0;

0.5000000000

> z=(1.25-cos(theta))^0.5;

$$(1.25 - \cos(\theta))^{0.5} = (1.25 - \cos(\theta))^{0.5}$$

> Qq:=1.0;

1.0

**> A:=plot(ay*(1.0-ay^2)/(1+ay^2-2.*ay*cos(theta))^1.5-
(Qq+ay),theta=0..Pi):**

**> B:=plot(k*(ay-cos(theta))*(exp(-k*(y-a)*z)-exp(-k*y*z))-k*(1-
(ay)*cos(theta))*(exp(-k*(y-a)*z))/(1+(ay)^2-
2.0*(ay)*cos(theta))+1-(ay)*cos(theta))*(exp(-k*(y-a)*z))-ay*(ay-
cos(theta))*(exp(-k*y*z))/(1.0+(ay)^2-2.*(ay)*cos(theta))^1.5+(-
k*(ay-cos(theta))+k*(1-ay*cos(theta)))*exp(-k*(y-a)*z)/z-1.0*exp(-
k*(y-a)*z),theta=0..Pi):**

> display(A,B);

k:=0.00824;

0.00824

ay:=1.0/2.0;

0.5000000000

```
a:=1.0;
```

```
1.0
```

```
y:=a/2.0;
```

```
0.5000000000
```

```
z:=(1.25-cos(theta))^0.5;
```

```
0.5
```

```
(1.25 - cos(theta))
```

```
Qq:=3.0;
```

```
A:=plot(ay*(1.0-ay^2)/(1+ay^2-2.*ay*cos(theta))^1.5-
```

```
(Qq+ay),theta=0..Pi):
```

```
B:=plot(k*(ay-cos(theta))*(exp(-k*(y-a)*z)-exp(-k*y*z))-k*(1-
```

```
(ay)*cos(theta))*(exp(-k*(y-a)*z))/(1+(ay)^2-
```

```
2.0*(ay)*cos(theta))+(1-(ay)*cos(theta))*(exp(-k*(y-a)*z))-ay*(ay-
```

```
cos(theta))*(exp(-k*y*z))/(1.0+(ay)^2-2.*(ay)*cos(theta))^1.5+(-
```

```
k*(ay-cos(theta))+k*(1-ay*cos(theta)))*exp(-k*(y-a)*z)/z-1.0*exp(-
```

```
k*(y-a)*z),theta=0..Pi):
```

```
display(A,B);
```

رابعاً في حالة لوح متصل بالأرض (قانون القوة العكسي و كولوم)

```
> with(plots):
```

```
> n:=1.1;
```

```
n := 1.1
```

```
> d:=1.0;
```

```
d:=1.0
```

```
>
```

```
B:=plot(1/(r^2+d^2)^(n/2+1),r=0.0..4.0,color=red,thickness=3,legend="yukawa n=1.1"):
```

```
>
```

```
A:=plot(1/(r^2+d^2)^(1.5),r=0.0..4.0,color=blue,thickness=3,legend="coulomb n=1"):
```

```
> n:=1.5;
```

```
n:=1.5
```

```
>
```

```
C:=plot(1/(r^2+d^2)^(n/2+1),r=0.0..4.0,color=black,thickness=3,legend="yukawa n=1.5"):
```

```
> n:=2.0;
```

```
n:=2.0
```

```
>
```

```
I:=plot(1/(r^2+d^2)^(n/2+1),r=0.0..4.0,color=green,thickness=3,legend="yukawa n=2.0"):
```

```
>
```

```
> n:=2.5;
```

```
n:=2.5
```

```
> d:=1.0;
```

```
d:=1.0
```

```
>
e:=plot(1/(r^2+d^2)^(n/2+1),r=0.0..4.0,color=orange,thickness=3,le
egend="yukawa n=2.5");
```

```
> n:=2.9;
```

```
n :=2.9
```

```
>
```

```
f:=plot(1/(r^2+d^2)^(n/2+1),r=0.0..4.0,color=brown,thickness=3,le
gend="yukawa n=2.9");
```

```
> n:=3.0;
```

```
n :=3.0
```

```
>
```

```
g:=plot(1/(r^2+d^2)^(n/2+1),r=0.0..4.0,color=yellow,thickness=4,le
gend="yukawa n=3.0");
```

```
> n:=3.5;
```

```
n :=3.5
```

```
>
```

```
h:=plot(1/(r^2+d^2)^(n/2+1),r=0.0..4.0,color=gray,thickness=4,le
gend="yukawa n=3.5");
```

```
> display(A,B,C,l,e,f,g,h);
```

خامسا كرة موصلية متصلة بالأرض (القوة العكسي و كولوم)

```
> with(plots):
```

```
> ay:=1.0/2.0;
```

```
0.5000000000
```

```
> n:=1.1;
```

```
1.1
```

```
>
```

```
> ay:=1.0/2.0;
```

```
0.5000000000
```

```
>
```

```
A := plot(n * (ay)^n * ((1 - ay * cos(theta)) - ay * (ay - cos(theta))) / (1  
+ ay^2 - 2.0 * ay * cos(theta))^(n + 2)/2), theta = 0.0 .. pi, color  
= red, thickness = 4, legend = "yukawa n=1.1") :
```

```
> B:=plot(ay*(1.-ay^2)/(1.+ay^2-
```

```
2.*ay*cos(theta))^1.5,theta=0..Pi,color=blue,thickness=4,legend="yukawa n=1.1"):
```

```
> display(A,B);
```

```
> ay:=1.0/2.0;
```

```
0.5000000000
```

```
> n:=1.5;
```

```
1.5
```

```
> A:=plot(n*(ay)^n*((1-ay*cos(theta))-ay*(ay-cos(theta)))/(1+ay^2-
```

```
2.0*ay*cos(theta))^(n+2)/2),theta=0.0..Pi,color=red,thickness=4,legend="yukawa n=1.5"):
```

```
> ay:=1.0/2.0;
```

```
0.5000000000
```

```
> B:=plot(ay*(1.-ay^2)/(1.+ay^2-
```

```
2.*ay*cos(theta))^1.5,theta=0..Pi,color=blue,thickness=4,legend="yukawa n=1.5"):
```

```

> display(A,B);
> ay:=1.0/2.0;
0.5000000000
> n:=2.9;
2.9
> A:=plot(n*(ay)^n*((1-ay*cos(theta))-ay*(ay-
cos(theta)))/(1+ay^2-
2.0*ay*cos(theta))^((n+2)/2),theta=0..Pi,color=red,thickness=4,
legend="yukawa n=2.9"):
> ay:=1.0/2.0;
0.5000000000
> B:=plot(ay*(1.-ay^2)/(1.+ay^2-
2.*ay*cos(theta))^1.5,theta=0..Pi,color=blue,thickness=4,legend="
yukawa n=2.9"):
> display(A,B);

```

سادسا في حالة كرة معزولة و مشحونة (القوة العكسي و كولوم)

```

> with(plots):
> ay:=1.0/2.0;
0.5000000000
> n:=1.1;
1.1
> Qq:=-3.0;
-3.0

```



```
> A:=plot(n*(ay)^n*((1-ay*cos(theta))-ay*(ay-  
cos(theta)))/(1+ay^2-  
2.0*ay*cos(theta))^((n+2)/2)+n*(Qq+ay^n),theta=0.0..Pi,color=red,  
thickness=2,legend="power law a/y=0.5 n=1.1 Qq=-3"):
```

```
> ay:=1.0/2.0;
```

```
0.5000000000
```

```
> B:=plot(ay*(1.-ay^2)/(1.+ay^2-  
2.*ay*cos(theta))^1.5,theta=0..Pi,color=blue,thickness=2,legend="Coulomb a/y=0.5 n=1.0"):
```

```
> display(A,B);
```

```
> ay:=1.0/4.0;
```

```
0.2500000000
```

```
> n:=1.1;
```

```
1.1
```

```
> Qq:=-3.0;
```

```
-3.0
```

```
> A:=plot(n*(ay)^n*((1-ay*cos(theta))-ay*(ay-  
cos(theta)))/(1+ay^2-  
2.0*ay*cos(theta))^((n+2)/2)+n*(Qq+ay^n),theta=0.0..Pi,color=black,  
thickness=2,legend="power law a/y=0.25 n=1.1 Qq=-3"):
```

```
> ay:=1.0/4.0;
```

```
0.2500000000
```

```
> B:=plot(ay*(1.-ay^2)/(1.+ay^2-  
2.*ay*cos(theta))^1.5,theta=0..Pi,color=green,thickness=2,legend=  
"Coulomb a/y=0.25");
```

```
> display(A,B);
```

```
> ay:=1.0/2.0;
```

```
0.5000000000
```

```
> n:=1.1;
```

```
1.1
```

```
> Qq:=-1.0;
```

```
-1.0
```

```
> A:=plot(n*(ay)^n*((1-ay*cos(theta))-ay*(ay-  
cos(theta)))/(1+ay^2-  
2.0*ay*cos(theta))^((n+2)/2)+n*(Qq+ay^n),theta=0.0..Pi,color=re  
d,thickness=2,legend="power law a/y=0.5 n=1.1 Qq=-1.0");
```

```
> ay:=1.0/2.0;
```

```
0.5000000000
```

```
> B:=plot(ay*(1.-ay^2)/(1.+ay^2-  
2.*ay*cos(theta))^1.5,theta=0..Pi,color=blue,thickness=2,legend="  
Coulomb a/y=0.5 n=1.0");
```

```
> display(A,B);
```

```
> ay:=1.0/4.0;
```

```
0.2500000000
```

```
> n:=1.1;
```

```
1.1
```

```
> Qq:=-1.0;
```

-1.0

```
> A:=plot(n*(ay)^n*((1-ay*cos(theta))-ay*(ay-  
cos(theta)))/(1+ay^2-  
2.0*ay*cos(theta))^((n+2)/2)+n*(Qq+ay^n),theta=0.0..Pi,color=bl  
ack,thickness=2,legend="power law a/y=0.25 n=1.1 Qq=-1.0"):  
> ay:=1.0/4.0;
```

0.2500000000

```
> B:=plot(ay*(1.-ay^2)/(1.+ay^2-  
2.*ay*cos(theta))^1.5,theta=0..Pi,color=green,thickness=2,legend=  
"Coulomb a/y=0.25 n=1.0"):
```

```
> display(A,B);
```

```
> ay:=1.0/2.0;
```

0.5000000000

```
> n:=1.5;
```

1.5

```
> Qq:=-1.0;
```

-1.0

```
> A:=plot(n*(ay)^n*((1-ay*cos(theta))-ay*(ay-  
cos(theta)))/(1+ay^2-  
2.0*ay*cos(theta))^((n+2)/2)+n*(Qq+ay^n),theta=0.0..Pi,color=re  
d,thickness=2,legend="power law a/y=0.5 n=1.5 Qq==1.0"):  
> ay:=1.0/2.0;
```

0.5000000000

```
> B:=plot(ay*(1.-ay^2)/(1.+ay^2-  
2.*ay*cos(theta))^1.5,theta=0..Pi,color=blue,thickness=2,legend="'  
Coulomb a/y=0.5 n=1.0'):
```

```
> display(A,B);
```

```
> ay:=1.0/4.0;
```

```
0.2500000000
```

```
> n:=1.5;
```

```
1.5
```

```
> Qq:=-1.0;
```

```
-1.0
```

```
> A:=plot(n*(ay)^n*((1-ay*cos(theta))-ay*(ay-  
cos(theta)))/(1+ay^2-  
2.0*ay*cos(theta))^((n+2)/2)+n*(Qq+ay^n),theta=0.0..Pi,color=bl  
ack,thickness=2,legend="'power law a/y=0.25 n=1.5 Qq=-1.0'):
```

```
> ay:=1.0/4.0;
```

```
0.2500000000
```

```
> B:=plot(ay*(1.-ay^2)/(1.+ay^2-  
2.*ay*cos(theta))^1.5,theta=0..Pi,color=green,thickness=2,legend=  
"Coulomb a/y=0.25 n=1.0'):
```

```
> display(A,B);
```

```
> ay:=1.0/2.0;
```

```
0.5000000000
```

```
> n:=2.9;
```

```
2.9
```

```
> Qq:=-1.0;
```

-1.0

```
> A:=plot(n*(ay)^n*((1-ay*cos(theta))-ay*(ay-  
cos(theta)))/(1+ay^2-  
2.0*ay*cos(theta))^((n+2)/2)+n*(Qq+ay^n),theta=0.0..Pi,color=re  
d,thickness=2,legend="power law a/y=0.5 n=2.9 Qq=-1.0"):  
> ay:=1.0/2.0;
```

0.5000000000

```
> B:=plot(ay*(1.-ay^2)/(1.+ay^2-  
2.*ay*cos(theta))^1.5,theta=0..Pi,color=blue,thickness=2,legend="'  
Coulomb a/y=0.5 n=1.0'"):
```

```
> display(A,B);
```

```
> ay:=1.0/4.0;
```

0.2500000000

```
> n:=2.9;
```

2.9

```
> Qq:=-1.0;
```

-1.0

```
> A:=plot(n*(ay)^n*((1-ay*cos(theta))-ay*(ay-  
cos(theta)))/(1+ay^2-  
2.0*ay*cos(theta))^((n+2)/2)+n*(Qq+ay^n),theta=0.0..Pi,color=bl  
ack,thickness=2,legend="power law a/y=0.25 n=2.9 Qq=-1.0"):  
> ay:=1.0/4.0;
```

0.2500000000

```
> B:=plot(ay*(1.-ay^2)/(1.+ay^2-
2.*ay*cos(theta))^1.5,theta=0..Pi,color=green,thickness=2,legend=
"Coulomb a/y=0.25 n=1.0"):
```

```
> display(A,B);
```

```
> ay:=1.0/2.0;
```

```
0.5000000000
```

```
> n := 1.1;
```

1.1

```
> Qq := -2.0;
```

-2.0

```
> A := plot(n*(ay)^n*((1-ay*cos(theta))-ay*(ay*cos(theta)))/(1
+ ay^2-2.0*ay*cos(theta))^(n+2)/2 + n*(Qq + ay^n), theta
= 0.0 ..pi, color = red, thickness = 2, legend
= "power law a/y=0.5 n=1.1 Qq=-2.0") :
```

```
> ay == 0.5;
```

0.5

```
B := plot(ay*(1.-ay^2)/(1.+ay^2-2.*ay*cos(theta))^1.5, theta = 0
> ..pi, color = blue, thickness = 2, legend
= "Coulomb a/y=0.5 n=1.0") :
```

```
> DISPLAY(A,B);
```

5.5 Reference

- [1] Cavendish H 1773 the Electrical Researches of the Honourable Henry Cavendish ed J C Maxwell (Cambridge:Cambridge University Press, 1879)pp 104–13.
- [2] Maxwell J C 1873 A Treatise on Electricity and Magnetism3rd edn (New York: Dover, 1954) pp 80–6.
- [3] Kobzarev I Y and Okun L B 1968 Usp. Fiz.Nauk.95 131–7Kobzarev I Y and Okun L B 1968 Sov. Phys. Usp. 11 338–41(Engl. Transl.)
- [4] Goldhaber A S and Nieto M M 1971 Rev. Mod. Phys.43 277–96.
- [5] Chibisov G V 1976 Usp. Fiz.Nauk.119 551–5Chibisov G V 1976 Sov. Phys. Usp. 19 624–6 (Engl. Transl.)
- [6] Goldhaber A S and Nieto M M 1976 Sci. Am. 234 86–96.
- [7] Byrne J C 1977 Astrophys. Space Sci. 46 115–32.
- [8] Jackson J D 1975 Classical Electrodynamics 2nd edn(New York: Wiley) pp 5–9.
- [9] Proca A 1936 J. Phys. Radium Ser. VII 7 347–53Proca A 1937 J. Phys. Radium Ser. VII 8 23–8.
- [10] De Broglie L 1940 La Méchanique Ondulatoire du Photon, Une Nouvelle Théorie de Lumière vol 1 (Paris: Hermann)pp 39–40.
- [11] Asseo E and Sol H 1987 Phys. Rep. 148 307–46.
- [12] Kronberg P P 1994 Rep. Prog. Phys. 57 325–82Kronberg P P 2002 Phys.Today 55 40–6.
- [13] Williams E R, Faller J E and Hill H A 1971 Phys. Rev. Lett.26 721–4Williams E R, Faller J E and Hill H A 1970 Bull. Am. Phys.Soc. 15 586–7 Williams E R 1970 PhD Thesis Wesleyan University, Middletown, CT Soc. 15 586–7Williams E R 1970 PhD Thesis Wesleyan University, Middletown, CT.
- [14] Chernikov M A, Gerber C J, Ott H R and Gerber H J 1992Phys. Rev. Lett.68 3383–6.

- [15] Lakes R 1998 Phys. Rev. Lett. 80 1826–9.
- [16] Luo J, Tu L-C, Hu Z-K and Luan E-J 2003 Phys. Rev. Lett.90 081801.
- [17] Feinberg G 1969 Science 166 879–81.
- [18] Schaefer B E 1999 Phys. Rev. Lett. 82 4964–6.
- [19] Fischbach E, Kloor H, Langel R A, Lui A T Y and Peredo M1994 Phys. Rev. Lett 73 514–17.
- [20] Davis L, Goldhaber A S and Nieto M M 1975 Phys. Rev. Lett.35 1402–5.
- [21] Ryutov D D 1997 Plasma Phys. Control. Fusion 39 A73–82.
- [22] Gintsburg M A 1963 Astron. Zh. 40 703–9Gintsburg M A 1964 Sov. Astron. AJ 7 536–40 (Engl. Transl.)
- [23] Patel V L 1965 Phys. Lett. 14 105–6.
- [24] Hollweg J V 1974 Phys. Rev. Lett. 32 961–2.
- [25] Barnes A and Scargle J D 1975 Phys. Rev. Lett.35 1117–20.
- [26] deBernadis P, Masi S, Melchiorri F and Moleti A 1984Astrophys. J. 284 L21–22.
- [27] Williams E and Park D 1971 Phys. Rev. Lett. 26 1651–2.
- [28] William R.Smythe, Static and Dynamic Electricity, 3rd ed., revised printing (Hemisphere,New York,1989).
- [29] This was noted by Max Abraham and Richard Becker, Classical Theory of Electricity and Magnetism, 2nd ed. (Hafner, New York, 1949); our derivation is based on Jeffrey Gima's unpublished Reed College senior thesis (1993).
- [30] W.R. Smythe "Charged Right Circular Cylinder,"J.App1.Phys.27, 917-920(1956). See also Ref.2, Sec.5.39.
- [31] - T.T.Taylor."ElectricPolareizability of Short Right Circular Conducting Cylinder,"J.Res.NBS 64,135-143(1960).
- [32] W.R.Smythe "Charged Right Circular Cylinder," J.App1.Phys.33, 2966-2967(1962).
- [33] W.R.Smythe, Ref.2, p.209.

- [34] Neyenhuis, B., Christensen, D. and Durfee, D.S. (2007) Testing Nonclassical Theories of Electromagnetism with Ion Interferometry. *Physical Review Letters*, **99**, 200401. <http://dx.doi.org/10.1103/PhysRevLett.99.200401>.
- [35] Tu, L.-C. and Lou, J. (2004) Experimental Tests of Coulomb's Law and the Photon Rest Mass. *Metrologia*, **41**, S136- S146.
- [36] Spencer, R.L. (1990) If Coulomb's Law Were Not Inverse Square: The Charge Distribution Inside a Solid Conducting Sphere. *American Journal of Physics*, **58**, 385-390. <http://dx.doi.org/10.1119/1.16179>.
- [37] Griffiths, D.J. and Uvanovic, D.Z. (2001) the Charge Distribution on a Conductor for Non-Coulombic Potentials. *American Journal of Physics*, **69**, 435-440. <http://dx.doi.org/10.1119/1.1339279>.
- [38] Jackson, J.D. (1975) Classical Electrodynamics. 2nd Edition, Wiley, New York.
- [39] Griffiths, D.J. (1999) Introduction to Electrodynamics. 3rd Edition, Prentice-Hall, Upper Saddle River.